Optimising microfluidic preparation of lipid sponge phase nanoparticles for biomolecule encapsulation

Owais Khalil

2023-06-15

Lund University, LTH

Chemical Engineering Department

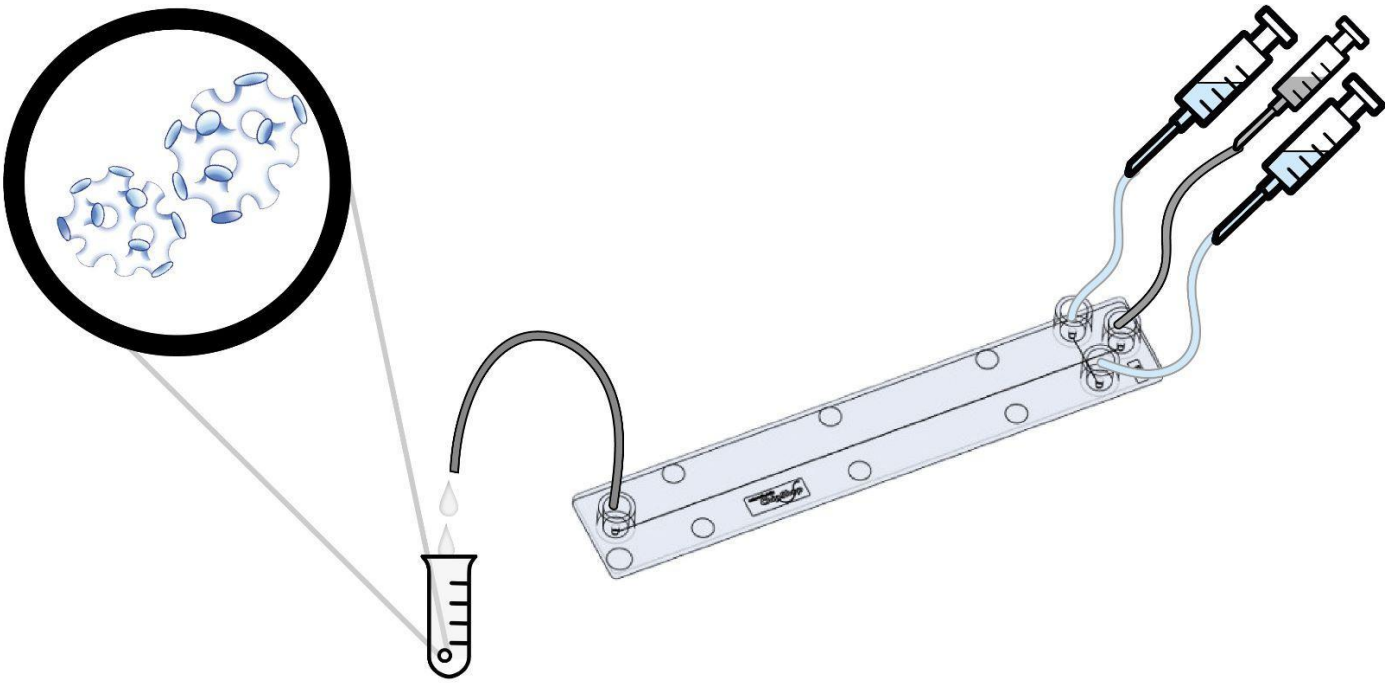

LUND UNIVERSITY | LTH FACULTY OF ENGINEERING

Abstract

Drug delivery with lipid nanoparticles, especially sponge phase lipid nanoparticles (LNP), has been well studied because of its ability for drug encapsulation and transferring the drug through the cell membrane. The sponge phase LNP formulation could be affected by the molecular structure of the lipid, the temperature, pH, dilution, the buffer, and addition of a stabiliser. This project aimed to replace the sonication method with microfluidics, because the sonication damages the sample by using ultrasound waves. However, in microfluidics more parameters were involved in the formulation, the total flow rate, and the lipid/buffer flow ratio. In this study, a mixture of mono-, di- and triglycerides and polysorbate 80 were used to investigate the formulation of sponge phase LNP by a microfluidic device. The effect of flow rate, flow ratio, stabilizer concentration, buffer and pH were studied to optimise the sponge phase LNP formulation method. Protein encapsulation was also tested to see how it would affect the size and structure of the LNPs.

The formulation method used a T-crossed channel chip where the channel has a rectangular shape, 140x200 µm, with three inputs and one output. A statistical experimental design by the software Design Expert was done to plan the project and decide the different sample preparation conditions. The effect of the buffer was studied by comparing the formulation in milli-Q water, tris(hydroxymethyl)aminomethane (TRIS) buffer at pH=7.2 and pH=8.9, and in phosphate buffer (PB) at pH=7.0. The protein encapsulation was tested with different protein concentrations. The size and the zeta potential of the LNP were measured by dynamic light scattering (DLS), and the structure of the LNP was determined by small-angle X-ray scattering (SAXS). In addition, some samples have been imaged in transmission electron microscope (cryo-TEM).

The size measurements of the LNP were fitted into a model that describes the effect of the parameters, total flow rate, and final lipid concentration that depended on the flow ratio and the concentration of the P80 as a stabiliser. According to the model, a high flow rate decreased the particle size, a high P80 concentration helped forming smaller particles, and a larger flow ratio led to lower lipid concentration and smaller particles. However, the pH also influenced the size where pH=7 helped forming smaller particles than pH=8.9. Furthermore, TRIS and phosphate buffer formed smaller particles than milli-Q water and they had clearer signals for the sponge phase. Even the encapsulation showed to influence the size and the phase of the LNP. High protein concentration disturbed the formulation of the sponge phase and led to bigger particles. Despite all, the microfluidic method showed its ability to form sponge phase LNP with different big sizes.

Sammanfattning

Läkemedelstransportering med lipidnanopartiklar (LNP), särskilt svampfas lipidnanopartiklar, har varit intressanta på grund av dess möjlighet att inkapsla läkemedel och överföra läkemedlet genom cellmembranet. Svampfas LNP formuleringen kan påverkas av lipidens molekylära struktur, temperaturen, pH-värdet, utspädningen, bufferten och existerandet av en stabilisator. Projektets syfte var att ersätta ultraljudsformuleringsmetoden med mikrofluidik, eftersom ultraljud skulle skada provet genom de inskickade energifulla ultraljudsvågor. I mikrofluidik system var fler parametrar involverade i formuleringen, den totala flödeshastigheten och lipid/buffertflödesförhållandet. I denna studie undersöktes blandningar av olika monooleat lipider och polysorbat 80 för att formulera svampfas LNP med hjälp av en mikrofluidik system. Effekten av flödeshastighet, flödesförhållande, stabilisatorkoncentration, buffert och pH studerades för att optimera LNP-formuleringsmetoden med svampfas. Proteininkapsling testades också för att se hur det skulle påverka storleken och strukturen på LNP.

Formuleringsmetoden använde ett T-korsat kanalchip där kanalen har en rektangulär form, 140x200 µm, med tre ingångar och en utgång. En statistisk experimentell design av programvaran Design Expert gjordes för att planera projektet och bestämma de olika provberedningsvillkoren. Genom resultatet studerades effekten av bufferten genom att jämföra formuleringen i milli-Q vatten, tris(hydroximetyl)aminometan (TRIS) buffert vid pH=7,2 och pH=8,9, och i fosfatbuffert (PB) vid pH=7,0. Proteininkapslingen testades med olika proteinkoncentrationer. Storleken och zetapotentialen för LNP mättes med dynamisk ljusspridning (DLS), och fasen för LNP bestämdes med liten vinkelröntgenspridning (SAXS). Dessutom har några prover avbildats i transmissionselektronmikroskop (cryo-TEM).

Storleksmätningarna av LNP monterades in i en modell som beskrev effekten av parametrarna, total flödeshastighet, slutlig lipidkoncentration som berodde på flödesförhållandet och koncentrationen av P80 som stabilisator. Enligt modellen minskade en hög flödeshastighet partikelstorleken, en hög P80-koncentration hjälpte till att bilda mindre partiklar, och ett mer signifikant flödesförhållande led till lägre lipidkoncentration och mindre partiklar. pH påverkade också storleken där pH=7 hjälpte till att bilda mindre LNP jämfört med pH=8,9. Dessutom bildade TRIS och fosfatbuffert mindre LNP än milli-Q-vatten och de hade tydligare signaler för svampfasen i SAXS mättningarna. Även proteininkapslingen visade sig påverka storleken och fasen av LNP. Hög proteinkoncentration störde formuleringen av svampfasen och ledde till större partiklar. Trots allt visade mikrofluidik metoden sin förmåga att bilda svampfas LNP med olika stora storlekar.

List of Abbreviations

LNP – Lipid nanoparticles

DGMO – Diglyceryl monooleate

GMO – Glyceryl monooleate

P80 – Polysorbate 80

TRIS – Tris(hydroxymethyl)aminomethane

PB – Phosphate buffer

DLS – Dynamic light scattering

PDI – Polydispersity index

SAXS – Small angle X-ray scattering

Cryo-TEM – Cryogenic transmission electron microscope

List of Figures

Figure 12. The plotting curves for the characterisations of LNP by SAXS. The measurements were run a month after the LNP formulation. The arrows point to the peaks. The blur curve is for the LNPs in milli-q water, yellow curve in TRIS buffer at pH=8.9, green curve in TRIS buffer at pH=7.2 and the red curve in PB at pH=7.0.

Figure 13. The SAXS patters of the protein encapsulated LNP with different protein concentration. The arrows point to the peaks.

Figure 14. Two images on the same sample but at different magnifications. The images show the sponge phase where the particle´s inside is in disordered for the sponge phase and ordered for the cubic phase. The elongated structures are caused by the sample plotting and have nothing to do with the LNPs.

Figure 15. The cryo-TEM images. a) and b) are images of the protein encapsulated LNP with 1.6 mg protein/ml formulated at 300 µl/min. c) is an image on LNP formulated in milli-Q water from the buffer effect tests.

List of Tables

Contents

1. Introduction

Cell membranes consist of a lipid bilayer and proteins, where the lipids are assembled to form the cell membrane with a bilayer structure. Non-lamellar phases of lipids have an important role in transport of substances and remodelling processes in the membrane, for example, the hexagonal phase is the base of the mitochondrial membrane fission and the swollen cubic phase in the butterfly wing gives the photonic crystals and colour. Cubic phases of highly curved lipid assemblies are also found in Golgi and endoplasmic reticulum where there is a high surface area to volume ratio, which also leads to an increase in the membrane stress, the hydrophobicity, and the capacity for protein transport. Vesicles are structures consisting of a sphere of lipid bilayer that is surrounded by and encapsulates water. Therefore, these structures have been used in drug delivery and biosensing applications because of their ability for substance encapsulation [1].

Lipid nanoparticles (LNP) are getting more interesting for their application in encapsulation due to their stability, internal structure, and their tuneable properties. The lipid nanoparticles can have different phases depending on the dilution, temperature, pH, kind of lipids and the existence of stabilizers. These phases can include bicontinuous cubic phase, discontinuous micellar cubic phase, and hexagonal phase. The sponge phase has a similar structure as the bicontinuous cubic phases, but it is more disordered. It is an efficient structure for encapsulation, because it has a large surface to volume ratio, and it is built by a single lipid bilayer that forms a network of intertwining and unconnected water channels [1].

In this thesis, the formation of 40/60 diglycerol monooleate/glycerol monooleate-50 nanoparticles with sponge phases by diluting the lipid mixture via microfluidics at different conditions is optimised. The size of the lipid nanoparticles produced from this method will be compared to the ones formed by sonication. The particle size and the polydispersity index will be measured using dynamic light scattering (DLS) and small angles X-ray scattering (SAXS) and the flow of the mixing in the microfluidic will be watched in an optics microscope.

The reason behind this project is to replace the sonication method, which damages the sample by using ultrasound waves, and to replace the conventional dispersion method that takes a long time and requires big amounts of material. While with microfluidics a small amount of product can be produced in a safe way for the sample, and with continuous production. In addition, the effect of polysorbate 80 (P80) as a stabiliser will be studied and the effect of tris(hydroxymethyl)aminomethane (TRIS) and phosphate buffer (PB) in different pH will be compared with milli-Q water. The LNP will be used to encapsulate protein and the effect of the encapsulation on the size and structure of the LNPs will also be studied. The main question of the project is how do the parameters of the microfluidics influence the particle size and phase, and do the buffer, pH and protein encapsulation affect the LNPs?

2. Background

2.1 Dispersion and particle structures

Dispersions are mixtures of particles in a continuous phase of the same or different state. For example, liquid particles in a gas phase or oxide particles in metal alloy phase. The dispersion mixture is homogeneous if the particles are stable and will not aggregate, like metal alloy, and it is heterogeneous when the particle has the tendency to aggregate or settle, like oil in water [2]. In pharmaceutical research, the particles are usually amphiphilic lipids dispersed in water to form lipid particles. Lipids are amphiphilic molecules where they have a hydrophilic side called the polar head and a hydrophobic side called the non-polar tail [2]. This type of molecule is usually called a surfactant, see lipid structure in Figure 2.

Therefore, when the surfactant is mixed with water, the hydrophilic head prefers to interact with the water molecules, while the hydrophobic chains interact with each other forming lipid particles where the hydrophilic heads are on the surface and the hydrophobic chains are gathered inside the particle [2]. The formation of lipid particles occurs when the concentration of the surfactant in water is at the critical micelle concentration (CMC) or higher, otherwise the surfactant would be dissolved in the continuous phase. Most lipids have a low solubility in water, however, the lipids can form different liquid crystalline phases with different water content. Depending on the concentration of the surfactant or the lipid in water as well as their molecular structure, different phases could be formed in the lipid particles, as Figure 1 shows.

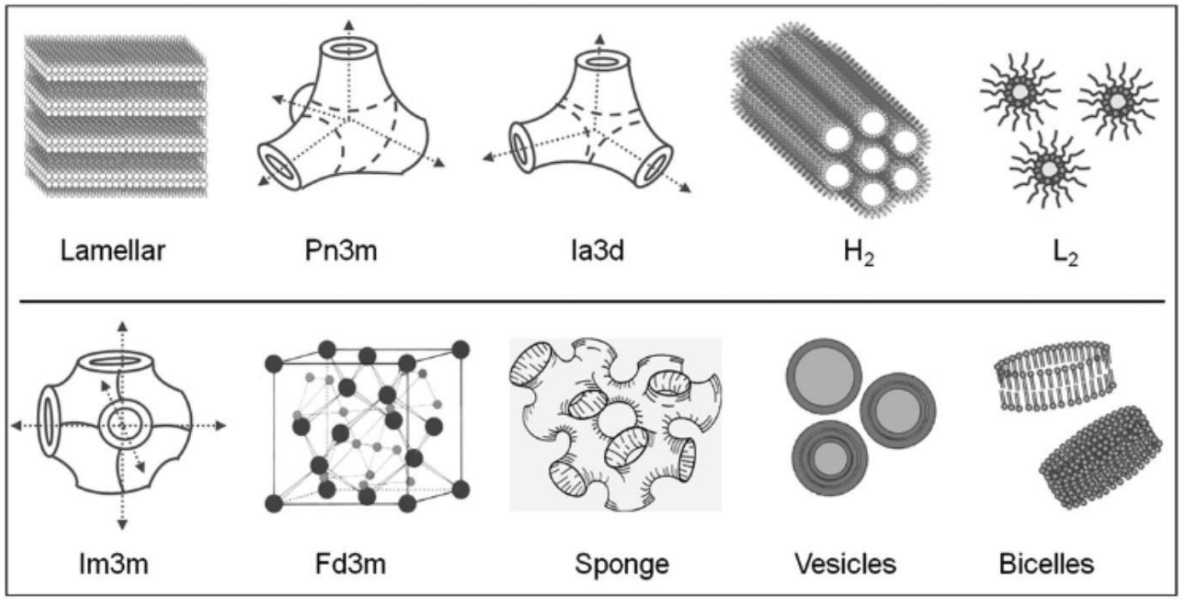

Figure 1. The different phases of lipid particles in water. The upper row are the phases that monoolein can form in water. While the lower row are the phases that form in the presence of other additives to stabilise the structure. [3]

However, the phase and the size of the lipid particles are affected by the solvent properties and the occurrence of a stabilizer. The hydrophobic effect is the driving force of the lipid self-assembly. This will drive the lipid phase to minimise the interaction area between the hydrophobic tail and the polar solvent or maximize it if the solvent is non-polar [3]. Therefore,

the solvent can affect the particle size and shape. Regarding the particle phase, different phases are stable at different concentrations, but some phases can be stabilized by a stabilizer like polysorbate 80 (P80) that has a bulky hydrophilic head.

The different phases in Figure 1 are favoured for different lipids depending on the chemical structures of the lipid molecule. The molecular structure of the lipid can be described with a geometric shape. This shape forms a phase that gives the best suitable structure to that shape. As Figure 2 shows, lipids with bulkier polar heads, type 1, tend to form positive curvature bilayer or oil/water dispersion [3]. While the lipids with the bulky non-polar tail, type 2, will form a negative curvature bilayer or w/o dispersion. Depending on how big the polar and non-polar parts are, the packing parameter can be different [3]. Bigger packing parameter indicates that the lipids will be closer to each other in the parking structure compering to the low packing parameter.

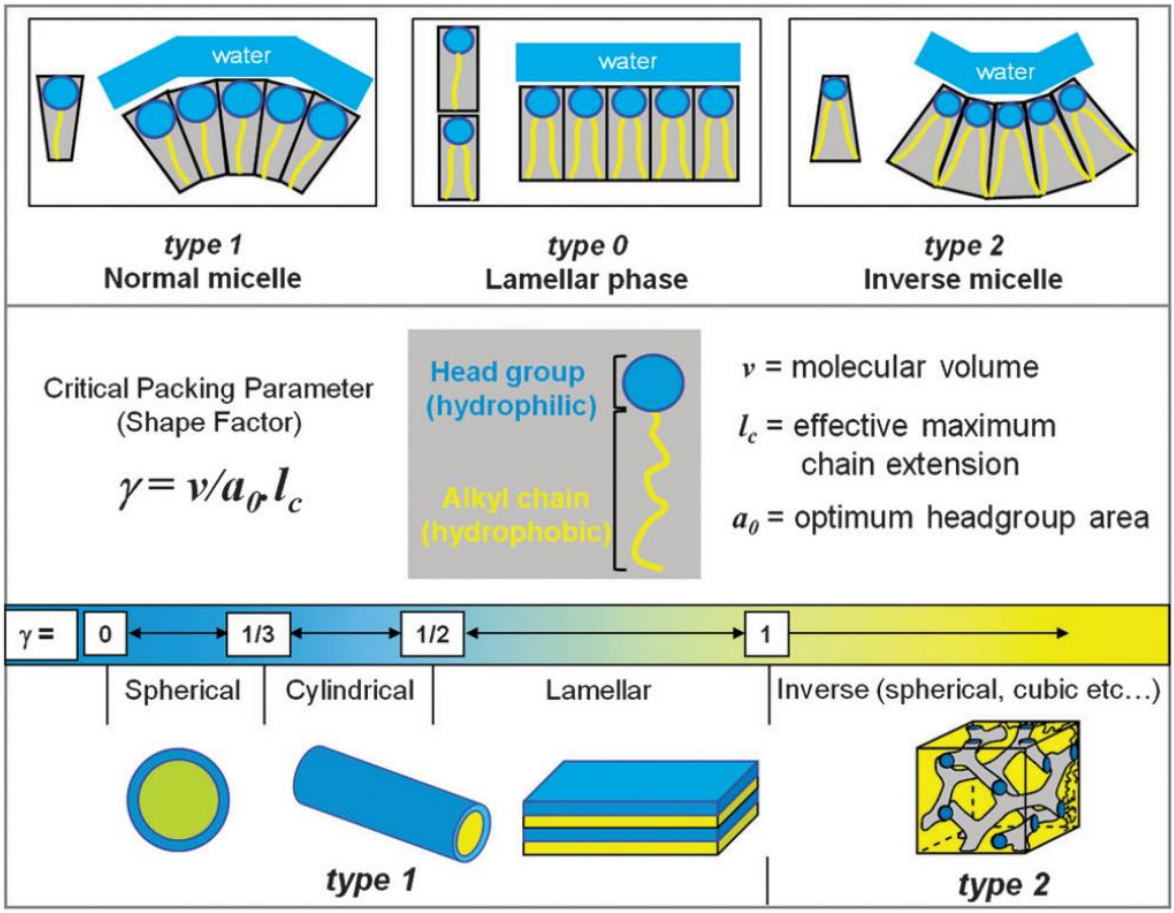

Figure 2. The molecular packing of the lipids can cause different phases depending on the shape and structure of the molecule. The packing parameter indicates how close the lipids are in the structure. [3]

2.2 Monooleates

Monooleates are fatty acid ester molecules formed by esterification between glycerol and oleic acid. Glyceryl monooleate (GMO) is an amphiphilic molecule where the glyceryl is the hydrophilic head, and the acyl chain is the hydrophobic tail. GMO has very low solubility in water, $\cong 10^{-6}$ M [5], even if it has a polar head, but is soluble in alcohol, oil, and petroleum [3].

To make the hydrophilic head bulkier, another glycerol molecule can attach to the glyceryl by an ether bond and form diglyceryl monooleate (DGMO). On the other hand, if the hydrophobic tail needs to be bulkier, more oleic acid molecules can bind to the glyceryl by an ester bond to get one or two more hydrophobic tails, see the molecular structures in Figure 3. In this study a mixture of glycerides with different numbers of hydrophobic tails is used. This specific mixture is called GMO-50, which contains glyceryl monooleate, glyceryl dioleate and glyceryl trioleate.

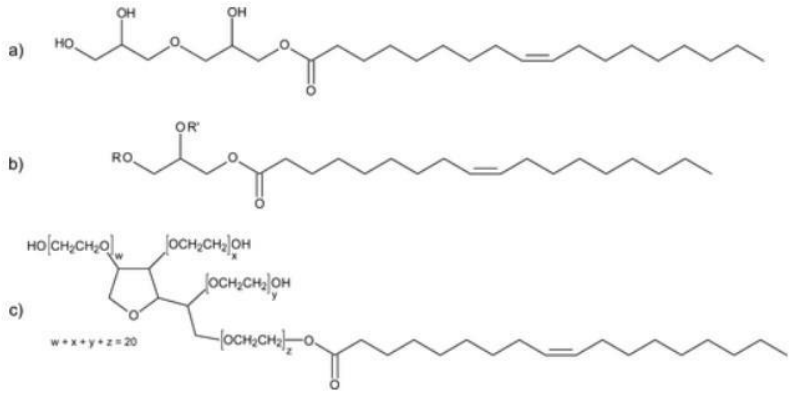

Figure 3. The chemical structure of, a) diglyceryl monooleate (DGMO), b) glyceryl monooleate (GMO), where R and R´ are either a hydrogen or carbon chains bonded with ester bond, and c) polysorbate 80 (P80).[6]

At low water content, i.e., concentrated GMO, a lipid crystalline lamellar phase is favoured where the bilayers of lipids are ordered. At higher water content of 20-50%, the GMO tends to form bicontinuous cubic phases such as the Ia3d phase, but if the water content increases, the Pn3m phase starts to form [5]. However, high dilution of the cubic phase could change the ordered lamellae to a disordered structure, like the sponge phase [5]. It is very hard to form the sponge phase with GMO in water, but instead it can be mixed with other lipids and with the addition of a stabilizer to form faster and more stable sponge phase particles. Figure 4 views how sponge phase LNP looks like.

A mixture of 40 wt% DGMO and 60wt% GMO-50 (40/60 DGMO/GMO-50) has been proven to help form the sponge phase. Because of the larger polar head of DGMO, it increases the limit of swelling, and the mixture of GMO-50 drives the formation of swollen reverse structures, because of the bulkier hydrophobic tails [6]. This helps to form bigger channels and smaller surface curvature in the structure. The addition of polysorbate 80 (P80) enhances the formation of structures with lower curvature by lowering the packing parameter, see Figure 2, because of the large head group in P80, and thus stabilizes the formation of swollen phases [6]. Figure 4 shows a cross section of how the lipids are organised in the bilayer to form the water channels inside the structure.

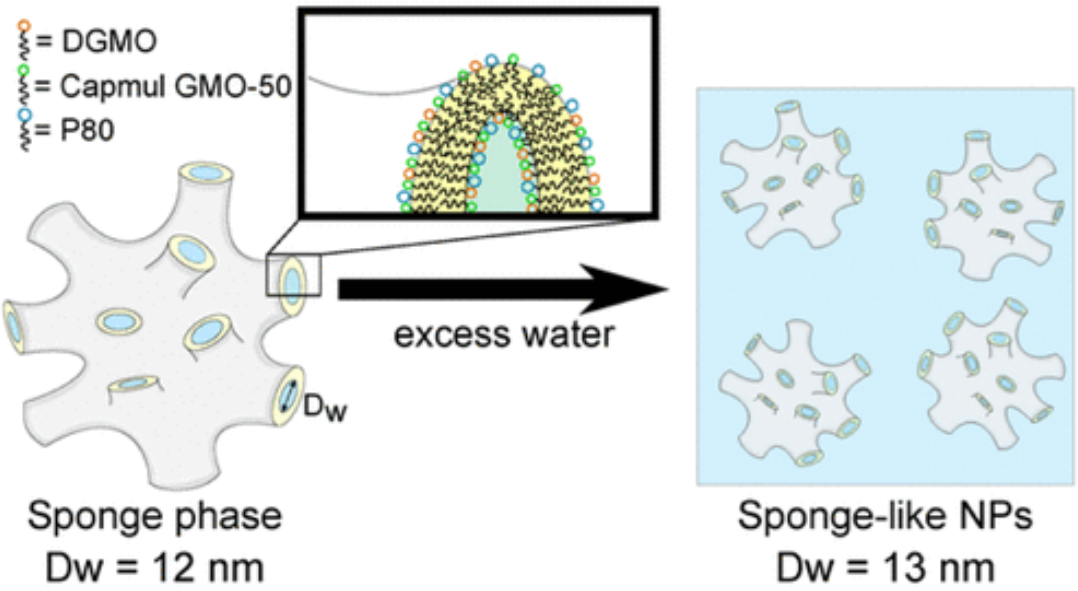

Figure 4. A cross section of the bilayer of sponge phase LNP. [6]

2.3 Formulation methods

2.3.1 Conventional method

Usually, the method used to prepare lipid nanoparticles starts by mixing a certain amount of the lipids in the buffer. Then, the lipids are dispersed in the buffer by ultrasonication. The process goes on until no lipid lumps are seen. The ultrasonication breaks up the agglomerations and disperses the lipids into particles. Sonication time and energy are important because more time means that more energy is transferred to the lipids, and this could damage the lipids and lead to phase change [7].

2.3.2 Microfluidics

Microfluidics is a system refers to the flowing of small amount of liquids in a very small channel, tens, or hundreds of micrometres in size. Mixing and transporting liquids in microfluidics can allow the opportunity to study the control of the product formulation and the diffusion of the molecule. Due to the small consuming amount of liquids, microfluidics consumes less energy and can be applied by automation using AI devices.

Dispersion of LNPs can also be made by mixing the buffer with the lipid solution in microfluidics using a channel chip. Microfluidics is a simple method for the formulation of LNP with easy setup and many samples can be made in a short time. Microfluidics has been used effectively to synthesise size controlled LNPs [8]. The lipid is usually dissolved in an organic solvent, and it mixes in the channel chip with the buffer where LNPs are formulated. A group from Hokkaido University have been investigating LNP formulation using a microfluidic device with a baffle structure [8]. They dissolved the lipids in ethanol and mixed it with a buffer in a Y-crossed channel chip where the lipid/ethanol solution meets the buffer and mixed inside the baffle structure of the chip with a total of 0.1-500 µl/min. To remove the ethanol from

the final LNP suspension, they used dialysis overnight in a NaCl-solution. They have shown that the size of the LNP produced by the microfluidics is smaller than the ones by the conventional method. Furthermore, a higher total flow rate produces smaller LNPS. They have been using a baffle device, which is different from the one used in this project. T-crossed channel chip has no baffles, see Figure 5, it is longer and smaller in channel size. Therefore, a range of different total flow rates, 50-150 µl/min, will be investigated to form LNPs with different weight concentrations, 0.5-1.5 wt%, depending on the flow ratio between lipid and buffer.

2.4 Analysing methods

2.4.1 DLS

Dynamic light scattering (DLS) is an analytical technique to determine the zeta potential and the size distribution of nanoparticles by measuring the elastic light scattering. Light is scattered either elastically with no energy exchange with the surrounding, or inelastically when the photon exchanges energy with the surrounding and the wavelength of the scattered light will be different. The shape and the interaction of the particles can affect the intensity of the scattered light. The light intensity decreases when the particles have repulsive interactions, while it increases when they have interactive interactions in between [9]. This is why the samples must be diluted to prevent the effect of the interactions. Because of the Brownian motion and diffusion of molecules, the instantaneous intensity is time-dependent, where the intensity varies with time due to how quick the fluctuation of the material density is. Smaller particles, like nanoparticles or molecular solutions, diffuse faster which makes the intensity fluctuation rapid. Conversely, with bigger particles, hundreds of nanometres or micrometres in size, the intensity fluctuation occurs at longer time scales because of the slower diffusion [9]. Then by correlating the rate of intensity fluctuation, the translational diffusion coefficient can be calculated and used in the Stokes-Einstein equation, see Equation 1, to determine the particle size and the polydispersity of the particles [9].

$$d_H = \frac{kT}{3\pi\eta D} \tag{1}$$

From the size distribution of the particles, the polydispersity index can be determined. If the PDI has a low value, less than 0.3, means that the LNPs in the sample are monodisperse and the LNPs have smaller size distribution. Monodispersed LNP are favoured to be able to rely on the size measurement.

DLS can also measure the zeta-potential of the LNP. Zeta-potential is the electric potential at the slipping/shear plane at the surface of a particle moving in electric field. Zeta-potential measures the potential difference between the electric double layer of the particle surface and the substances around it. This will give information about the charge of the surface [10]. The zeta-potential can be affected by the concentration of the particles, the pH, the buffer, and the ionic strength that can be interacted with the charged surface of the particles.

2.4.2 SAXS

Small angle X-ray scattering (SAXS) is a powerful technique for characterization of nanoparticles in a dispersion mixture. SAXS uses short wavelength, parallel and monochromatic X-rays that hit the nanoparticles in a dispersion mixture and scatter at small angle < 5° [11]. The scattering is affected by the topography of, interactions between and the element of the nanoparticles, heavier elements scatter more than lighter. The scattered X-rays are detected with a semiconductor plate where it measures the angle and the wavelength of the scattered X-rays. In addition, the intensity of the scattering is depending on the particle´s size and structure and by plotting the intensity against the momentum transfer, both the size and the structure of the particle can be determined [11]. The scattering angle (Θ) and the wavelength (λ) of the X-ray beam are used to calculate the momentum transfer (q) by equation 2 [11].

$$q = \frac{4\pi}{\lambda} sin\ sin\ (\Theta) \quad (2)$$

Then for sponge phase structure, the characteristic pattern should contain two peaks, the lower intensity peak, q≈0.06 $Å^{-1}$, corresponds to the sponge cell-cell correlation distance, while the higher intensity peak, q≈0.1 $Å^{-1}$, represents correlation bilayer in the sponge phase [12].

2.4.3 Cryo-TEM

Cryogenic transmission electron microscopy (cryo-TEM) works similarly to a conventional TEM where an electron beam is transmitted through the specimen and an image can be created from the intensity of the transmitted electrons. The main difference with cryo-TEM is that the samples are studied at the cryogenic temperature, which is usually the liquid-nitrogen temperature [13]. This technique is suitable for colloidal structure of dispersion where the shape, the size and the internal structure of the nanoparticles can be analysed.

3. Materials

Lipids: GMO-50, diglyceryl monooleate and polysorbate 80 (P80).

Chemicals: milli-Q water, ethanol, tris(hydroxymethyl)aminomethane (TRIS), hydrochloric acid (HCl), disodium hydrogen phosphate (Na_2HPO_4) and sodium dihydrogen phosphate (NaH_2PO_4).

Protein: Freeze dried aspartic protease.

4. Experimental methods

4.1 Standard dispersions

Standard dispersions were made to compare with the dispersions from microfluidics devices. First, stock solutions must be made by mixing 40 wt% DGMO and 60 wt% GMO-50 in three glass vials. P80 was added to vials with ratio of 70/30, 72.5/27.5 and 75/25 (lipid/P80), respectively. The final lipid composition of the mixtures (DGMO/GMO/P80) would be 28/42/30, 29/43.5/27.5 and 30/45/25 respectively, and they are called according to the composition of P80, for example 40/60 DGMO/GMO-50 30 wt% P80. The vials were left for 24 h on a roller mixer to dissolve homogeneously. Then, around 0.1 g of lipid mixture are weighted and mixed with 2 ml of a buffer as Table 1 shows. The lipids were dispersed in milli-Q water and TRIS buffer via sonication. The sonication carried out until all lipids were dispersed and the mixtures looked homogeneous.

The size of the lipid nanoparticles (LNP) and the polydispersity of the final dispersions were measured using DLS. While the lipid phase of the LNPs was determined using SAXS.

Table 1. The weighted amounts lipids and buffer for the formulation of the standard dispersions. The last column shows the sonication times required to form a homogenous mixture.

Lipid mixture	Weigh of lipids mixture (g)	Buffer (ml)	Sonication time (Pulse 01 01 01)
40/60 DGMO/GMO-50 25 wt% P80	0.0988	2 ml Milli-Q water	3 min at Ampl 30% 1 min at Ampl 35%
40/60 DGMO/GMO-50 25 wt% P80	0.1061	2 ml TRIS	5 min at Ampl 30%
40/60 DGMO/GMO-50 27.5 wt% P80	0.1060	2 ml Milli-Q water	3 min at Ampl 30% 1 min at Ampl 35%
40/60 DGMO/GMO-50 27.5 wt% P80	0.0988	2 ml TRIS	3 min at Ampl 30%
40/60 DGMO/GMO-50 30 wt% P80	0.1018	2 ml Milli-Q water	2 min at Ampl 30% 1 min at Ampl 35%
40/60 DGMO/GMO-50 30 wt% P80	0.1020	2 ml TRIS	2 min at Ampl 30% 1 min at Ampl 35%

4.2 Microfluidic dispersions

Stock solutions: The stock solutions of lipids were made by dissolving the lipid mixtures, the same lipid mixtures used for the standard dispersion with the different P80 concentration, in ethanol where lipid concentration is 3 wt%, see the weighted amounts in Table 2. Ethanol was chosen as a solvent for the lipids because the lipid can easily dissolve in ethanol, and it was also easy to separate the ethanol from the final dispersion by evaporating it.

Table 2. The weighted amount of lipid mixture and ethanol to form the lipid stock solutions. All the solutions contain 3 wt% lipid in ethanol with a total weight of 10 g.

Lipid mixture	Weigh of lipids mixture (g)	Ethanol (g)
40/60 DGMO/GMO-50 25 wt% P80	0.3004	9.7004
40/60 DGMO/GMO-50 27.5 wt% P80	0.3063	9.7035
40/60 DGMO/GMO-50 30 wt% P80	0.3014	9.6995

Microfluidics: The LNPs were formulated using the T-crossed channel chip to mix the lipid-ethanol with filtered water to increase the contact area between the lipids and the Milli-Q water where the diffusion occurs. The milli-Q water flowed from the two sides, while the lipid flows from the middle, see Figure 5 for further understanding. The three flow rates are controlled with pumps where the diameter of the syringes and the desired flow rates were controlled by the pumps. The flow ratio (lipid/buffer) was adjusted to achieve the desired concentration of the lipid in the produced dispersion mixture. A software, Design-Expert, was used to statistically design the experiment where the range of the parameters were defined, and it picked up the conditions that should be tested. The parameters were 1) total flow rate (50-150 µl/min), 2) lipid concentration (0.5-1.5 wt%) and 3) stabiliser concentration (25-30 wt%), Table 3 shows which conditions were tested. The software required a response value, which was the measured particle sizes of the samples. After each test, the channel chip was cleaned with two Milli-Q water flow (each 150 µl/min) and ethanol (250 µl/min) for 10 min, then 6 ml air are blown in every channel simultaneously.

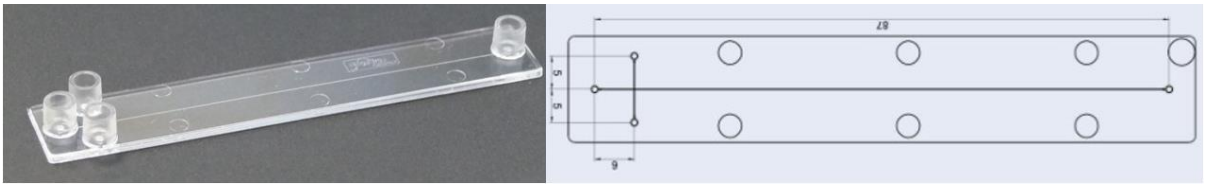

Figure 5. The T-crossed channel chip. The channel has a rectangular form where the height is 140 µm and the width is 200 µm [microfluidic-chipshop.com].

Table 3. The different conditions of the tests suggested by the Design-Expert software to model the relations between the parameters and the particle size.

Sample	Total Flowrate (µl/min)	C_{lipid} (wt%)	Flow ratio (Lipid/MQ)	C_{P80} (wt%)
1	50	0.5	1:5	27.5
2	150	0.5	1:5	27.5
3	50	1.5	1:1	27.5
4	150	1.5	1:1	27.5
5	50	1	1:2	25
6	150	1	1:2	25

7	50	1	1:2	30
8	150	1	1:2	30
9	100	0.5	1:5	25
10	100	1.5	1:1	25
11	100	0.5	1:5	30
12	100	1.5	1:1	30
13	100	1	1:2	27.5
14	100	1	1:2	27.5
15	100	1	1:2	27.5

To remove the ethanol from the dispersions, vacuum evaporation by a rotary evaporator was used at room temperature. The produced samples had different concentration of lipid as in Table 3, but all were diluted with milli-Q water to form a dispersion with 0.25 wt% lipids. Therefore, different samples were diluted with different but controlled factors. To determine the lipid content, 1 ml of the diluted samples were weighted and putted in the vacuum evaporator. The sample was weighted before and after the evaporation to be able to calculate the concentration of the lipid. The evaporation was carried out for 1 hour. The size and the polydispersity of the LNPs were measured in DLS and the phase structures were determined by SAXS.

4.3 Buffer effect

TRIS: tris(hydroxymethyl)aminomethane buffer was made by mixing 50 mM of TRIS-solution with 50 mM HCl-solution. The HCl-solution was dropped in the TRIS-solution while monitoring with a pH probe until the pH of the mixture became the desired one. Two TRIS buffers were made, one with pH=8.9 and the other had pH=7.2.

PB: phosphate buffer was prepared from 50 mM of Na_2HPO_4-solution mixed with NaH_2PO_4-solution. The amount of the mixed solution was controlled by measuring the pH of the mixture. NaH_2PO_4-solition was added until the pH=7.0.

The LNPs were then prepared by dispersing the lipid mixture with 25 wt% P80 in the microfluidics with 4 different buffers: milli-Q water, two TRIS buffers and PBS. For this step, a random condition was chosen to compare the buffer effect. The total flow rate for the chosen condition was 300 µl/min and the final lipid-concentrations were 2 wt%. Then both the particle size and the zeta potential of the LNP were measured in DLS in addition to the SAXS measurements.

4.4 Protein encapsulation

The protein aspartic protease was dissolved in MQ. Three protein solutions were made with different concentrations, 2, 3 and 4 mg/ml. The protein solutions were mixed with the lipid mixture via the T-crossed channel chip by the same method described above. The flow ratio was kept to 1:4, where the two protein solutions had a flow rate of 120 µl/min and the lipid mixture in ethanol was with 60 µl/min. This gives a total flow rate of 300 µl/min and a final

lipid concentration of 2 wt%. The protein concentrations depended on the protein concentration in milli-Q water and in the collected sample they are 1.6, 2.4 and 3.2 mg/ml respectively. The total flow rate was changed for the protein solution with 2 mg/ml to 500 µl/min but the flow ratio 1:4 kept the same. The lipid mixture used for the encapsulation was 30 wt% P80, because according to the literature, higher concentration of P80 helps forming the sponge phase [6]. Then the ethanol was evaporated by the same method for the optimization samples. The particle size of the encapsulated LNP was measured in DLS and SAXS after the evaporation of the ethanol.

4.4 Measurements

Optical microscope: The microscope was used to see the concentration profile of the lipid mixture and track the formulation of big lipid particles inside the channel.

DLS: The samples were diluted 100 times in buffer (MQ, TRIS or phosphate buffer depending on which buffer was used in the samples). The measurements were carried out at 25 ^{o}C with 120 s as an equilibrium time. The material was polystyrene latex, and the used cuvettes were the disposable cuvettes ZEN0040. The measurement angle is 173^{o} and each sample was measured five times. For the measurements of the zeta potential, the same dilution and installation were chosen but the cuvettes were disposable folding capillary cuvettes DTS1070.

SAXS: 100 µl of each sample was injected into the capillaries and putted in the SAXS-machine. The measurements took 2 hours and were done at room temperature, 25 ^{o}C, with the configuration method 22. The samples with the protein encapsulated LNPs were measured by Co-SAXS in MAX IV laboratory at 25 ^{o}C.

Cryo-TEM: A carbon film was discharged first to make it easier for a sample to stick to it. 4 µl of a sample dropped on the carbon film. An absorption filter came closer from the back side and absorbs the liquid phase from the sample. Then the carbon film with the sticked samples was immediately doped in liquid ethane to freeze it at -104 ^{o}C. The carbon film was then stored in liquid nitrogen. The sample transferred into the cryo-TEM to image the LNP.

5. Results and discussion

5.1 Standard dispersions

Table 4 shows the particle size of the LNP formulated by the conventional method with sonication. It is clearly seen the effect of P80 where it decreases particle size. This is because of the bulky hydrophilic head of P80 is enriched at the surface of the particle and helps to stabilise it. The larger amount of P80 can therefore stabilise a higher surface area, driving the formulation of smaller particles. At the same time, P80 helps form a positive curvature that can stabilise the formation of small channels inside the structure and formulate sponge phase LNP. The effect of P80 has been observed in both milli-Q water and in the TRIS buffer. By looking at the polydispersity index in Table 4, LNP in TRIS have lower polydispersity than the same sample in milli-Q water. This can depend on the increase in stability of the LNP by the buffer ions. But overall, the polydispersity in all the samples has values around 0.2-0.3, which are good values and indicates that samples are monodispersed, despite the polydispersity of the sample in the third row. Figure 6 shows the SAXS characterisations of the LNPs in the standard solution and all of them have the same shape with one broad peak, except for the sample with 25 wt% P80 in TRIS buffer that has a small peak at Q=0.05 $Å^{-1}$. This small peak means that there are some sponge phase LNPs in this sample. But otherwise, if there is only one peak, which is more likely to be corresponding to the correlation thickness of the lipid bilayer, it is not certain to say that these LNPs have sponge phase structure rather than vesicles. That could be due to the use of sonication to disperse the lipid in the buffers. The sponge phase usually exists in a limited concentration/composition regime of the phase diagram, and it is sensitive to temperature. Therefore, sonication can affect the structure via heating the LNPs by the sound waves and drive the phase change.

Table 4. The measuring data of the LNPs synthesized by the conventional method with sonication.

Lipid mixture	Buffer	Size (d. nm)	Polydispersity index	Phase
40/60 DGMO/GMO-50 25% P80	Milli-Q water	127.3±2.3	0.192±0.013	Vesicles-Sponge
40/60 DGMO/GMO-50 25% P80	TRIS 50 mM pH=8.9	140.2±3.5	0.104±0.008	Vesicles-Sponge
40/60 DGMO/GMO-50 27.5% P80	Milli-Q water	128.5±3.7	0.316±0.014	Vesicles-Sponge
40/60 DGMO/GMO-50 27.5% P80	TRIS 50 mM pH=8.9	132.5±4.1	0.164±0.011	Vesicles-Sponge
40/60 DGMO/GMO-50 30% P80	Milli-Q water	113.7±3.1	0.238±0.009	Vesicles-Sponge
40/60 DGMO/GMO-50 30% P80	TRIS 50 mM pH=8.9	126.3±2.2	0.163±0.011	Vesicles-Sponge

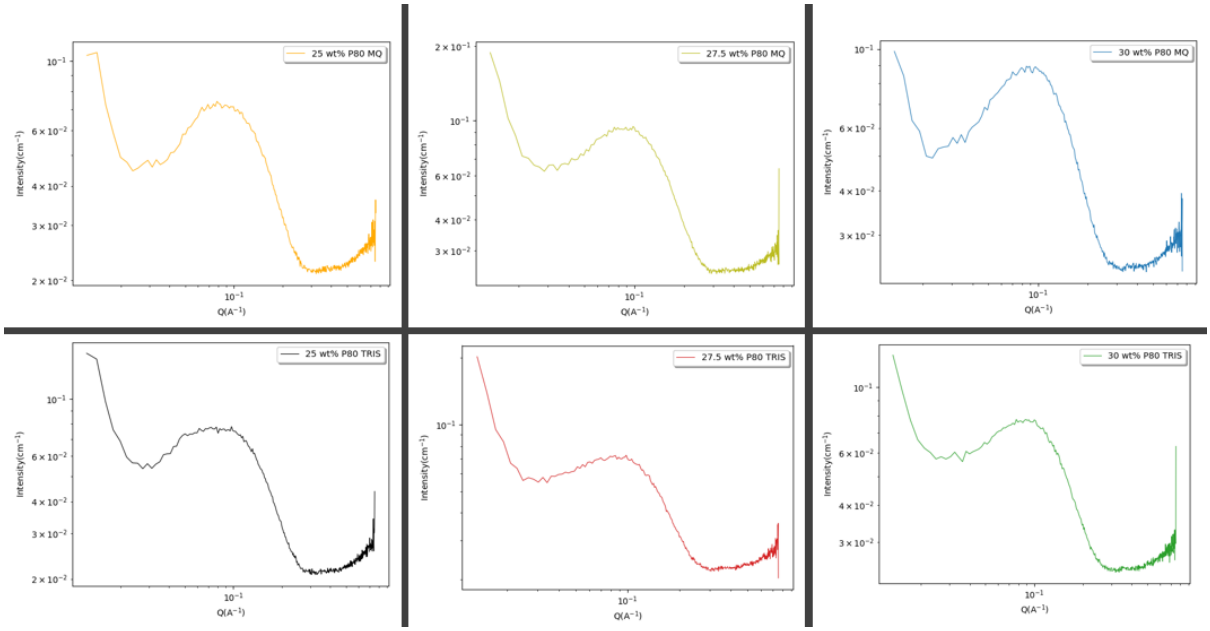

Figure 6. The SAXS characterisations plots for the LNPs in the standard dispersions.

5.2 Microfluidics optimization

The optimisation of the microfluidic was done statistically by running 15 different tests, as Table 3 shows, and measuring the size of the formulated LNPs. From Table 5, most of the samples had a low polydispersity index, less than 0.3, which means that the microfluidic can be used to prepare monodisperse LNPs since the size distribution of the LNPs is smaller with a low polydispersity index. The software suggested a quadratic model where there are terms that describe interactions between the parameters and even the square of the parameters. The model had to be modified by removing the two terms, (F^2) and ($[S]^2$), because their p-value was too high, which indicates the chance to get the null hypothesis where a random number occurs. The factor [S] is an essential parameter in the predicted model and cannot be removed, which is why it was considered as a significant term and was still in the model despite of its high p-value. The term (F[L]) was kept in the model and considered to be significant because it helped to increase the value of R^2.

Table 5. The measurements of the size and the polydispersity of the 15 samples. These data on the particle size were then used to fit a statistical model that described the effect of the different parameters.

Sample	Size (d. nm)	Polydispersity index
1	243±16.3	0.194±0.011
2	259±16.7	0.216±0.014
3	294±12.4	0.279±0.018
4	287±5.7	0.446±0.049
5	246±5.6	0.173±0.024
6	267±14.7	0.221±0.015
7	306±14.0	0.23±0.022
8	234±6.4	0.187±0.01

9	261±11.3	0.225±0.030
10	282±11.4	0.455±0.059
11	228±3.7	0.172±0.008
12	289±13.7	0.272±0.004
13	262±5.7	0.162±0.013
14	244±10.6	0.139±0.023
15	257±8.4	0.236±0.012

The measured size of the samples was used to fit a mathematical model that relates the parameter with size. Table 6 contains the terms needed to fit the model, some of them at significant terms and some are not. The p-value is the chance of having no effect of the parameter and this value is best when it below 0.05. The fitting model used only the significant terms and it has a p-value of 0.0014 which means that it is a significant fit and the R^2 is also high, near 95% chance to detect correctly. From Figure 7 shows that the measuring data follow the same trend as the model, despite the deviation from the line. To see more about the fitting model and the effect of each parameter, see Appendix A.

Table 6. The fitting data and the statistical effect of the different parameters. F stand for the total flowrate (µl/min), [L] for the final lipid concentration (wt%) that depends on the flow ratio and [S] is the composition of P80 in the lipids (wt%).

Source	**F-value**	**p-value**	
Model	17.27	0.0014	Significant
F	7.65	0.0326	Significant
[L]	75.02	0.0001	Significant
[S]	1.31	0.2959	Significant
F[L]	3.68	0.1035	Significant
F[S]	16.47	0.0067	Significant
[L][S]	8.72	0.0255	Significant
$[L]^2$	11.82	0.0138	Significant
F^2	0.325	0.3651	Not significant
$[S]^2$		0.6134	Not significant
Lack of fit	0.2977	0.8607	Not significant
Fit statistics:			
R^2 = 0.9527			
Adjusted R^2 = 0.8975			
Predicted R^2 = 0.7460			

The equation to predict the particles size (d) in nm is:

$$d = 254 - 6.63F + 23[L] - 3.17[S] + 6.5F[L] - 13.75F[S] + 12.92[L][S] + 12.96[L]^2 \qquad (3)$$

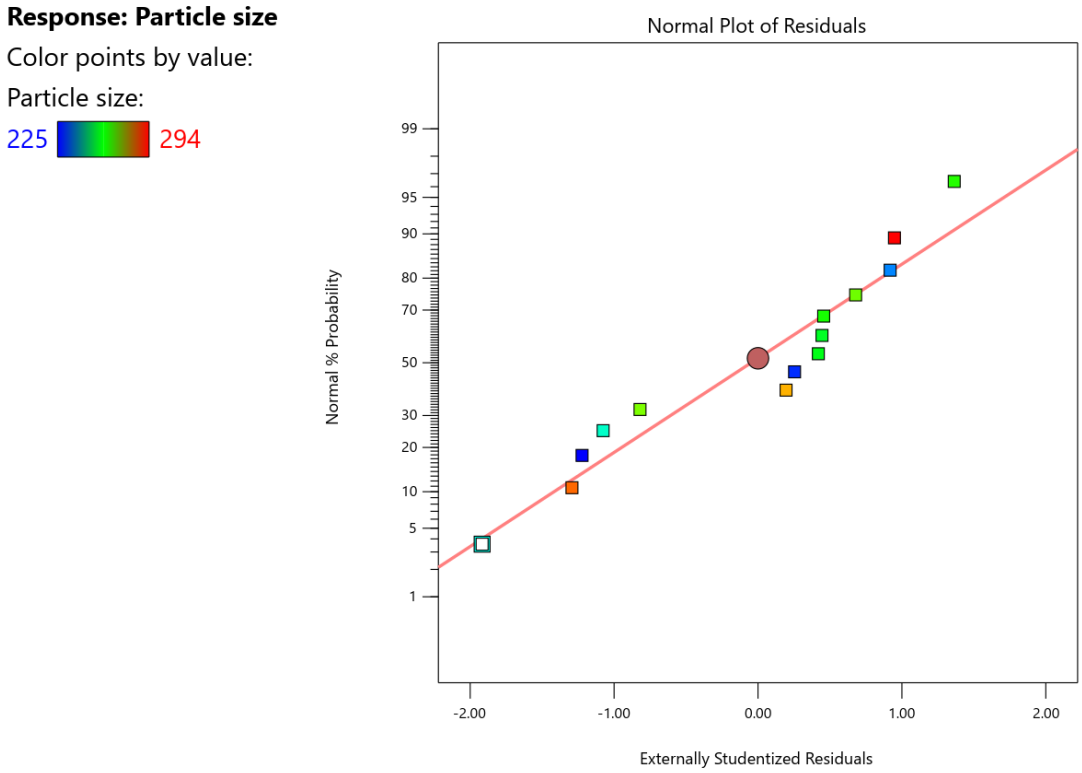

Figure 7. The particle size measuring data plotted with the predicted model to see how well the model fits with the experimental data. The big round, brown point is the centre point.

The microfluidics optimization is studied by statistically testing the relation between the different parameters of the synthesis method. The parameters were total flow rate (F), final lipid concentration ($[L]$) and stabilizer concentration ($[S]$) in the lipid mixture. The particle size was the response parameter to evaluate the effect of the parameter on the size and in case there is any relation between them. Equation (3) is the equation of the model fitted on the tests by the software Design-Expert. The model shows that the flow rate and the stabilizer decrease the size of the LNPs which is why these two parameters have a negative coefficient in the model. The effect of the P80 as a stabilizer in microfluidics formulation was expected and it agrees with the study by Valldeperas M. The existence of P80 decreases the thickness of the swollen bilayer [6]. This effect stabilises the formation of the sponge phase and smaller LNPs because P80 helps to form surface with positive curvature, which makes the packing parameter bigger [6].

Another study by Kimura N. [8] has proved that a higher total flow rate in microfluidics forms smaller particles. They were studying a microfluidic chip with baffles inside the channel, where the flow can generate turbulent movement at the end of each baffle and that is what makes the mixing more effective. However, in the T-crossed channel chip there are no baffles, even that the same effect of flow rate was detected. According to the model and the measuring data of the different tests, a higher flow rate decreases the size of the LNP. This is due to the short residence time in the channel that prevents the LNP from aggregating. The channel is thin and a flow rate of 50 µl/min means that the mixture spends 2.7 s in the channel and the higher the flow rate the shorter the residence time becomes. However, at slow

movement of the flows the LNP may have the chance to aggregate, which was proven by the forming of big particles inside the channel, see Figure 9.

As Figure 8 shows, the change in the thickness of the lipid flow corresponds to the diffusion of the lipids into the water, which causes the lipid flow to be broader at the end of the channel. This is also a sign that this is a good method to disperse lipids because it is clearly seen how the lipids are capable of diffusing into the buffer. Thus, the total flow rate affects the broadness of the concentration profile. The higher the flow rate the shorter the residence time will be, which means that the lipids will have less time to diffuse, and the dispersion will not be fully homogenous at the end of the channel. Another thing that should be mentioned, is that at every test with low flow rate, 50 µl/min, lipid lumps start to form inside the channel. They move slowly, break down and form again. Figure 9 is a series of images taken from a film that shows how these big particles are forming in the channel. Despite this, no lumps could be seen in the collected sample. This phenomenon was observed when the flow rate was 100 µl/min, but not as much as the 50 µl/min flow, and was never seen at 150 µl/min. This aggregation we see in Figure 9 was happening only inside the channel, and it seems more likely that these big particles are dispersed in the bulk phase in the tube.

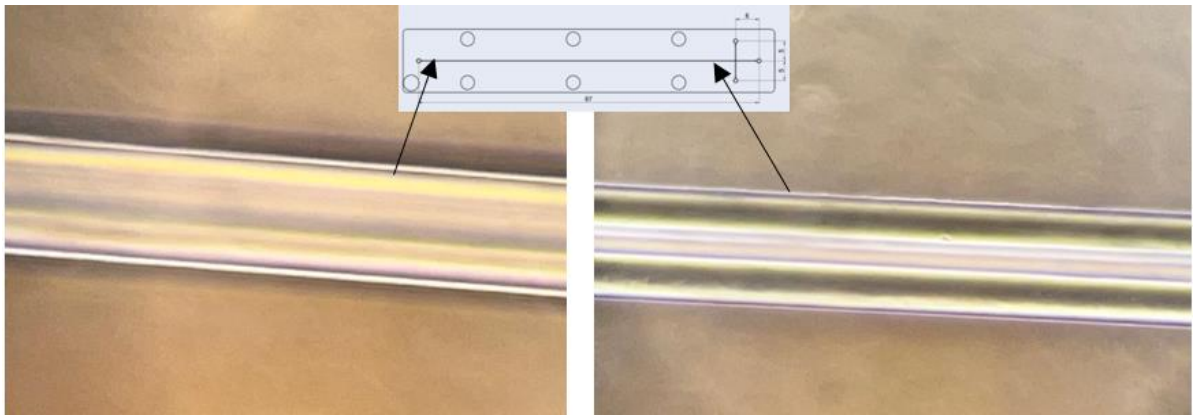

Figure 8. 40x magnification image on the channel chip. The change of the concentration profile of the lipids in milli-Q water along the channel chip. At the beginning of the channel, the lipid flow is thin in the middle in the image to the right. While at the end of the channel in the image to the left, the concentration profile is broader, and the mixture is more homogenous.

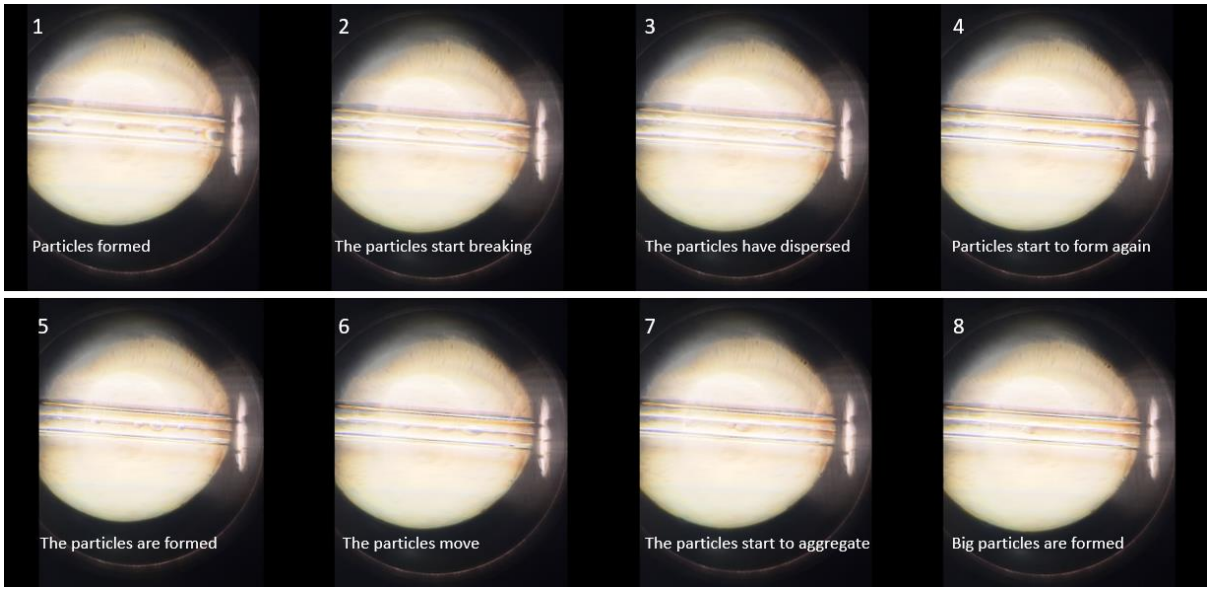

Figure 9. The movement, formulation and breaking of big lipid particles in the channel when the total flow rate was 50 µl/min. The time difference between image 1 to image 8 is 15 seconds on the same position in the channel.

The third parameter that had the strongest effect is the final lipid concentration or instead the flow ratio between the lipid mixture and water because it is the ratio that determines the final concentration. According to the results and the fitting model, a bigger flow ratio, which ends up with a lower lipid concentration, produces a smaller LNP, and this is caused by the T-crossed shape of the chip. As Figure 10a) and 10b) shows, the higher the flow ratio, the thinner the lipid flow becomes. The diagram in Figure 10c) is showing how the solutions flow beside each other. The lipid mixture feels the pressure from the buffer flows at the interface between the flows. But because of the minimal velocity of the lipid at the interface with the channel, the lipid mixture flow is squeezed at the middle where the mass diffusion is highest [14]. This explains why the mixture is not seen fully homogeneous from the optical microscope, see Figure 8. By the optical microscope, only the interface between the lipids and the channel are seen where the velocity of the lipid flow is close to zero. Therefore, the lipids at this interface diffuse very slowly into the buffer phase. This causes the aggregation of the lipids to form big particles at the interface with the channel and that what is shown in Figure 9. Furthermore, a higher flow rate causes higher pressure and will squeeze the lipid flow even more and the diffusion of the lipids will be faster and that forms smaller particles.

Figure 11 shows the SAXS characterisation of some of the samples prepared by using the lipid stock solution that was 10 wt % lipid in ethanol. The reason why these are the ones that are presented is because the time did not allow to measure every sample prepared. The samples in Figure 11 were prepared by higher flow rate and higher concentration than the samples used to make the model. Almost all the SAXS plots have two peaks, see where the arrows are pointing, which leads to the conclusion that most of the LNP produced in microfluidics are in sponge phase, no matter what flow rate or concentration they have. Compared to the standard dispersion, the LNP formulated by the microfluidics are clearly in the sponge phase, while this is not the case when the sonication was used in the standard dispersions. The

formulation of sponge phase LNP by microfluidics was a successful method with shorter time, no damaging risk, and no heating.

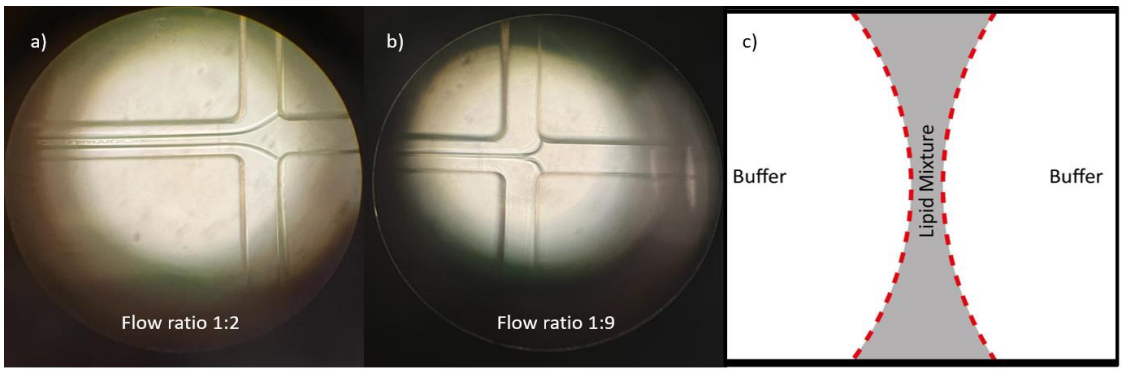

Figure 10. The meeting point of the water flows with the lipid mixture at the same total flowrate, 200 µl/mi, but at different flow ratio. c) is a cross section for the channel and it show the concentration profile of the lipid mixture flow through the channel.

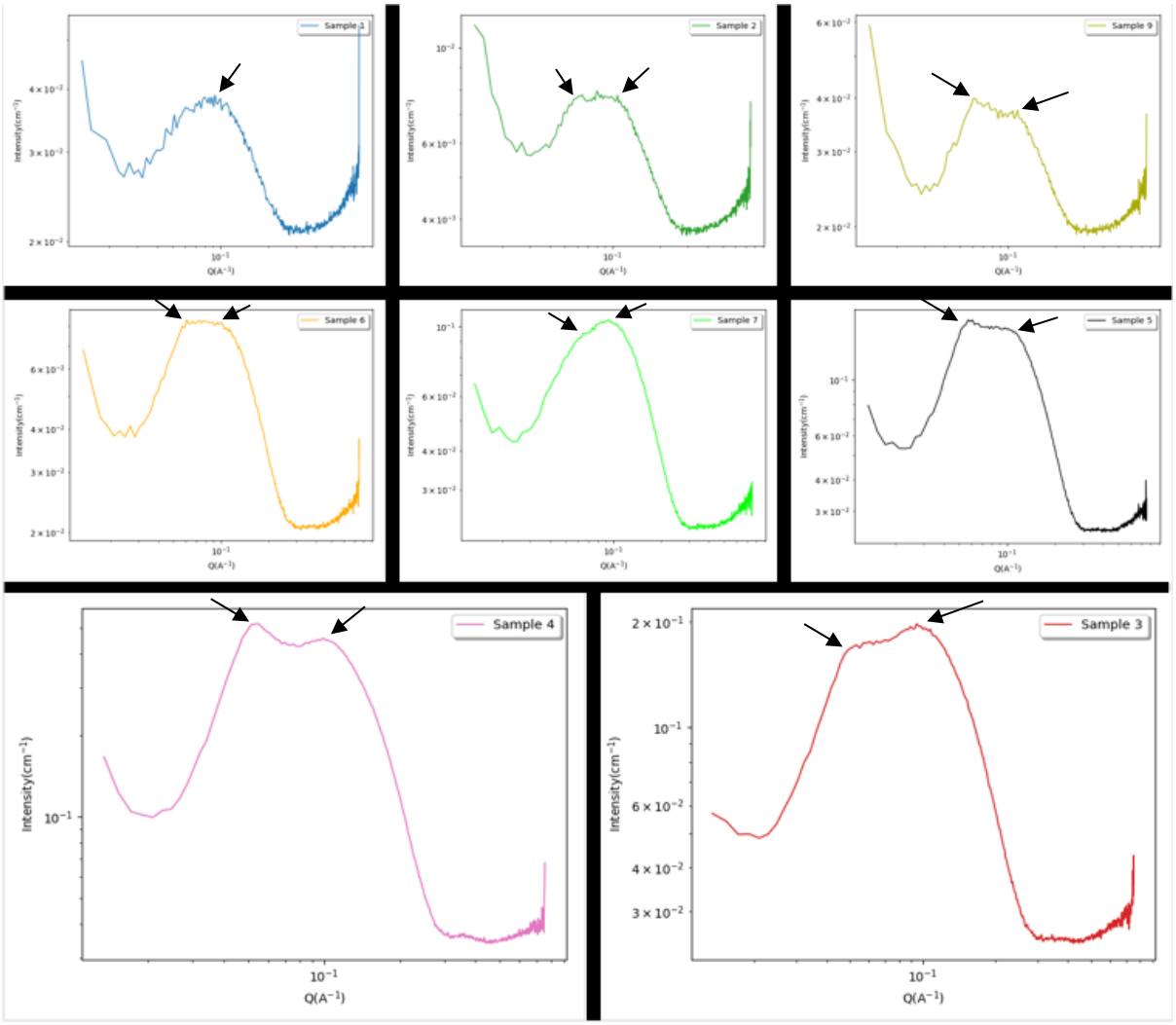

Figure 11. The SAXS plots for the characterisations of LNPs in some of the samples for the optimisation of the conditions by using 10 wt% lipid in ethanol stock solution. The conditions used to prepare sample 1-9 are the same as for the same samples number in Table 3. The first row are samples with 1.75 wt% lipid, the second row with 5 wt% lipid and the last row have 8wt% lipid. The arrows point to the peaks.

However, the method must be improved further to get full control over the particle size. Through the improvement of this method, different processes have been tested. In the beginning, dialysis and vacuum evaporation were compared to see which method removes the ethanol better. The comparison was done by measuring the size and the polydispersity index, which showed that vacuum evaporation leads to a smaller polydispersity index. The evaporation method was then improved by testing different ways with and without sample dilution before starting the evaporation using different evaporation times. According to DLS measurements, when the sample is diluted so that the lipid concentration is 0.25 wt% and then evaporate about half of the buffer, the polydispersity index is much smaller, which means that the samples have monodispersed LNPs. The data in Appendix B shows the measurements and the evaluation of the ethanol removal method. Even the lipid concentration in the stock solution was changed, 10 wt% lipid in ethanol was used first, but it was a high concentration where the size control was lost, which is why it was changed to 3 wt%. Higher flow rates were also tried out, and it was found that for flow rate 300-500 µl/min, the residence time in the channel was too short for the diffusion of the lipids, and that is why the size control over the LNP was lost. Despite the loss of the size control, sponge phase LNP were still created. Another parameter that is worth to be tested is the dimension of the channel because the concentration profile of lipid in the flow is also dependent on the size of the channel.

5.3 Buffer effect

The buffer is one of the important factors for the formulation and the stability of the LNP. The measurements of the LNP sizes and the polydispersity showed that the existence of ions and the value of pH has an influence on the size and the stability of LNPs. From Table 7, the LNPs in milli-Q water have the most negative zeta potential which means that the surface of the LNP is charged. Charged LNPs tend to repel each other which prevent the aggregation of the particles and therefore this repulsion increases the LNP´s stability. However, when there are ions in the solution, the charge of the surface becomes weaker, and the zeta potential becomes closer to zero. This explains the change in the polydispersity of the LNPs between the first measurement and the second one month after for the buffer samples. Because of the low zeta potential caused by the existence of ions, the LNP are more likely to aggregate to form bigger particles. That is why the polydispersity of the LNP in TRIS and PBS buffer gets higher, while for milli-Q water was mostly unchanged because of the better repulsion between the LNP which provide a higher stability.

However, when it comes to the particle size, pH around 7 and PBS buffer helps the formulation of smaller particles better than TRIS and milli-Q water at the same pH level. But it cannot be determined exactly how big this influence is because of the measuring method that DLS uses. DLS measures the hydrodynamic diameter of the LNP, including the electric layer that surrounds the particle's surface. Therefore, this diameter will be affected by adding a buffer. Depending on how big the ions are and how close they interact with the surface, the size could be different. The pH also seems to have an impact on the size, lower pH makes the particles smaller and generate a more stable sponge phase, see the SAXS measurements in

Figure 12. By measuring the zeta-potential of LNP in milli-Q water, it seems that the LNPs are negatively charged. The zeta-potential is closer to zero at lower pH, and this can be because of the protonation of the lipids. But in general, it could be concluded that the results show the trend of the buffer effect where PB and TRIS at pH around 7 helps synthesising smaller LNP. However, the stability of the LNPs is best in milli-Q water, because even after a month the polydispersity index and the particle size had not changed a lot.

Table 7. The measurement data of the LNP synthesised from lipid mixture 40/60 wt% of DGMO/GMO-50 with 25 wt% P80 in different buffers and the same flow rates (300 µl/min) and flow ratio (1:4). Size 1 and polydispersity index 1 are the measurements direct after the formulation, while size 2 and polydispersity index 2 are the measurements one month after the formulation on the same LNP.

Buffer	Size 1 (d. nm)	Polydispersity Index 1	Size 2 (d. nm)	Polydispersity Index 2	Zeta potential (mV)	Phase
Milli-Q water	239±3.5	0.213±0.009	264±4.4	0.218±0.02	-46.3±1.2	Vesicle-Sponge
TRIS 50 mM pH = 8.9	298±6.9	0.395±0.019	414±14	0.494±0.056	-36.1±1.8	Vesicle-Sponge
TRIS 50 mM pH = 7.2	227±3.3	0.360±0.018	360±5.1	0.403±0.044	-14.8±0.5	Sponge
PB 50 mM pH = 7.0	199±2.5	0.242±0.013	482±17	0.469±0.11	-15.9±1.1	Sponge

By analysing the characteristic scattering of LNPs by SAXS, see Figure 12, the high intensity peak is existed in all the samples which means these are lipid bilayers. According to older studies [11], the characteristic scattering pattern for sponge phase LNP should contain two peaks, which are clearly seen for the sample with PBS and TRIS with 50 mM at pH around 7. For TRIS at pH=8.9, there is a low intensity peak, which is not really at the right position, but it could mean that this is a sponge phase but not as strong signal as the other. However, in milli-Q water the sponge phase cannot be clearly defined because the lower intensity peak does not exist. PBS and TRIS at pH=7 provide the stability of the sponge phase even after the aggregation of LNPs. This is also a sign that the existence of positive ions in the buffer stabilises the sponge phase and does not only influence smaller particle size.

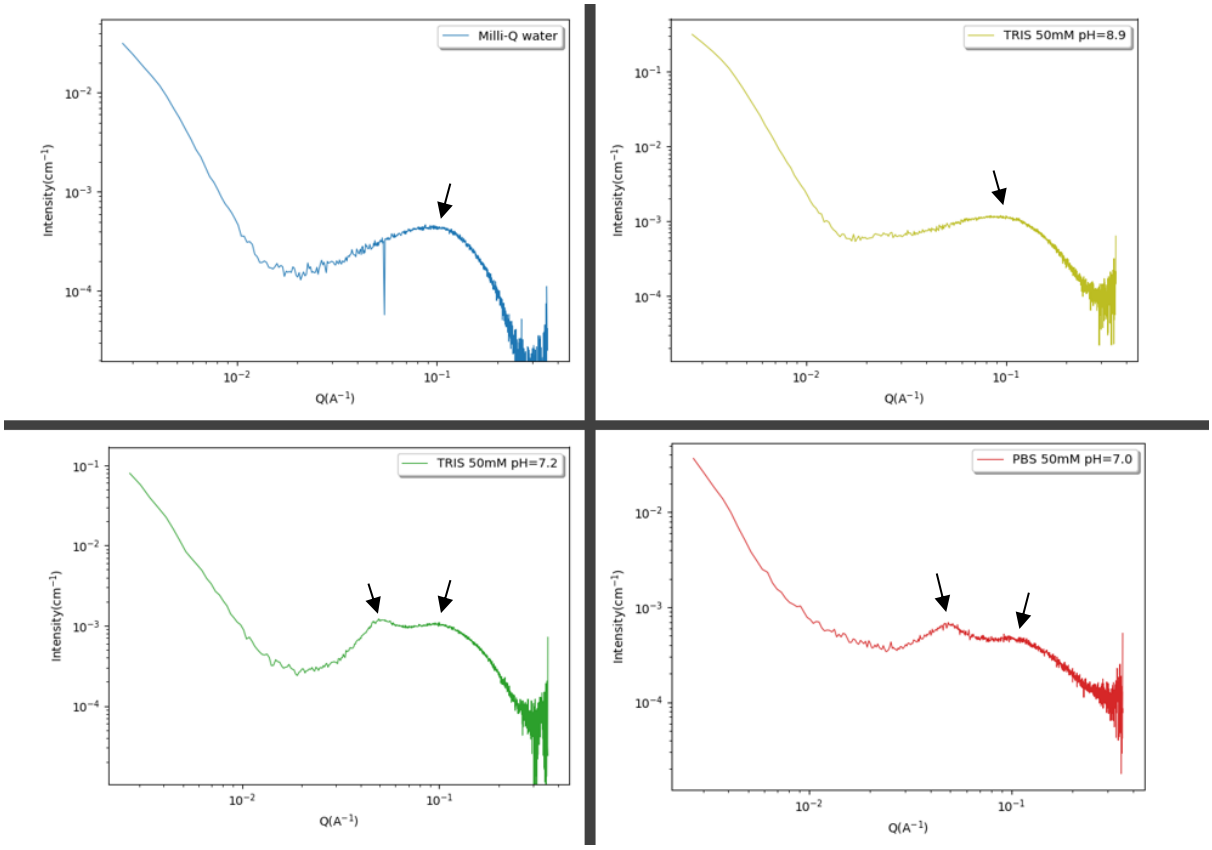

Figure 12. The plotting curves for the characterisations of LNP by SAXS. The measurements were run a month after the LNP formulation. The arrows point to the peaks. The blur curve is for the LNPs in milli-q water, yellow curve in TRIS buffer at pH=8.9, green curve in TRIS buffer at pH=7.2 and the red curve in PB at pH=7.0.

5.4 Protein encapsulation

The protein encapsulation is assumed to be occurring in microfluidics where the proteins move inside the water channel of the sponge phase LNPs when they are self-assembled. The particle size becomes bigger when the protein concentration is higher, this is because when the amount of the proteins is more, it becomes harder to encapsulate all the proteins. Therefore, the LNP self-assemble forming bigger particles to encapsulate more proteins or the proteins could stick on the surface of the LNP which could disturb the SAXS measurements. Because of that, the size control over the LNPs is lost when the protein concentration increases However, the same effect of the total flow rate is observed where it decreases the LNP size.

By analysing the protein encapsulated LNPs, the SAXS patterns of all the encapsulation samples tells that these LNP have vesicle phase. However, the peak of the diagrams is small compared to the other previous samples where the peak is more noticeable. This means the encapsulation has affected the formation of the particle structure and it is no longer a sponge phase. Although a small peak at around 0.1 Å is seen, which indicates that vesicles or another bilayer structure is existed.

Table 8. The protein encapsulation in LNP formed from a lipid mixture of 40/60 wt% of DGMO/GMO-50 with 30 wt% P80 in milli-Q water.

[Protein] (mg/ml)	Total flowrate (C)	Size (d. nm)	Polydispersity Index	Phase
20	500	260±7.7	0.230±0.013	Vesicles
20	300	268±2.6	0.225±0.009	Vesicles
30	300	347±11	0.287±0.012	Vesicles
40	300	327±9.2	0.311±0.035	Vesicles

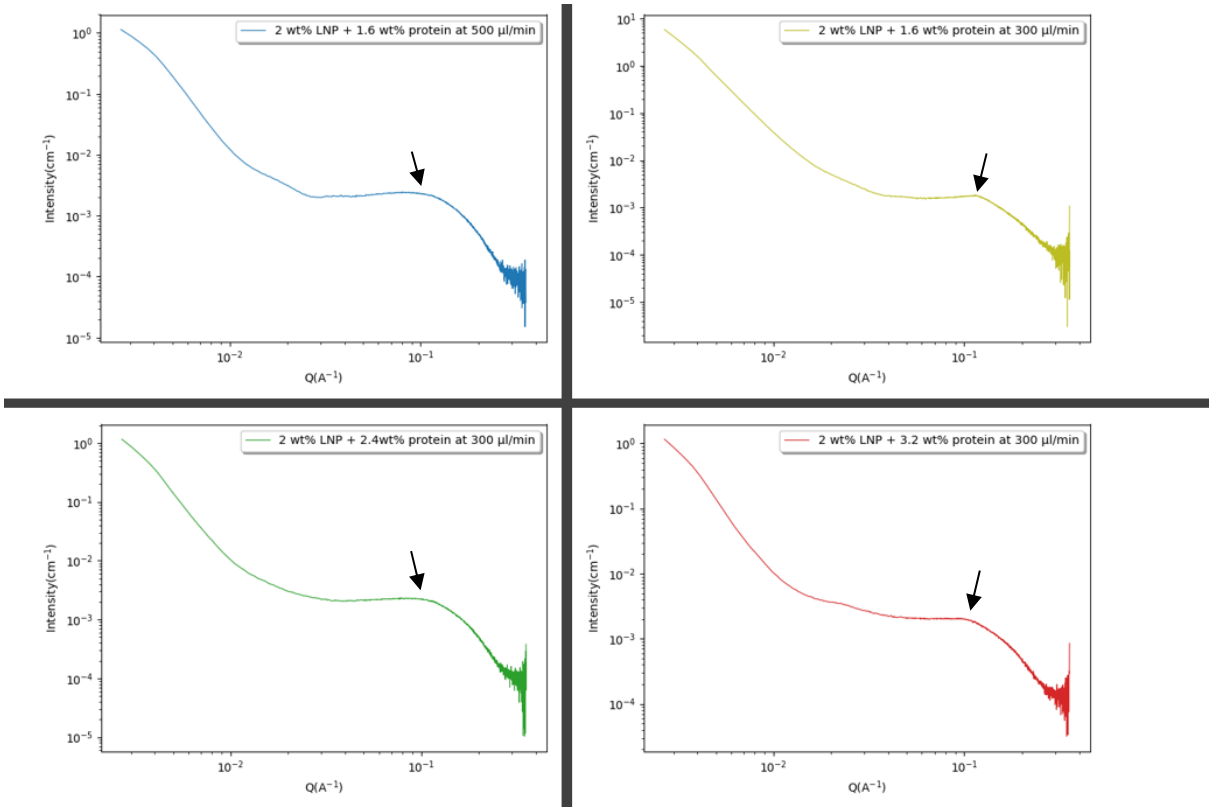

Figure 13. The SAXS characterisation patters of the protein encapsulated LNP with different protein concentration. The arrows point to the peaks.

5.5 cryo-TEM imaging

The final step was to look at the sponge phase LNPs. The sample number 5 from the from Table 5 was chosen to be imaged in cryo-TEM, because it was proven by the SAXS measurement that it has sponge phase LNP. The difference between cubic and sponge phase is that the cubic phase structure has an order, while sponge phase structure is disordered. In Figure 14, the difference can be seen, the intensity dots in the cubic phase particles are arranged in lines to each other comparing to the sponge phase particles that seems to be disordered and the intensity dots are randomly organised. Even the edges of the sponge phase LNP are rough, see the high magnified image in Figure 14, and means that the surface of the LNP is not continuous as in the cubic phase LNP.

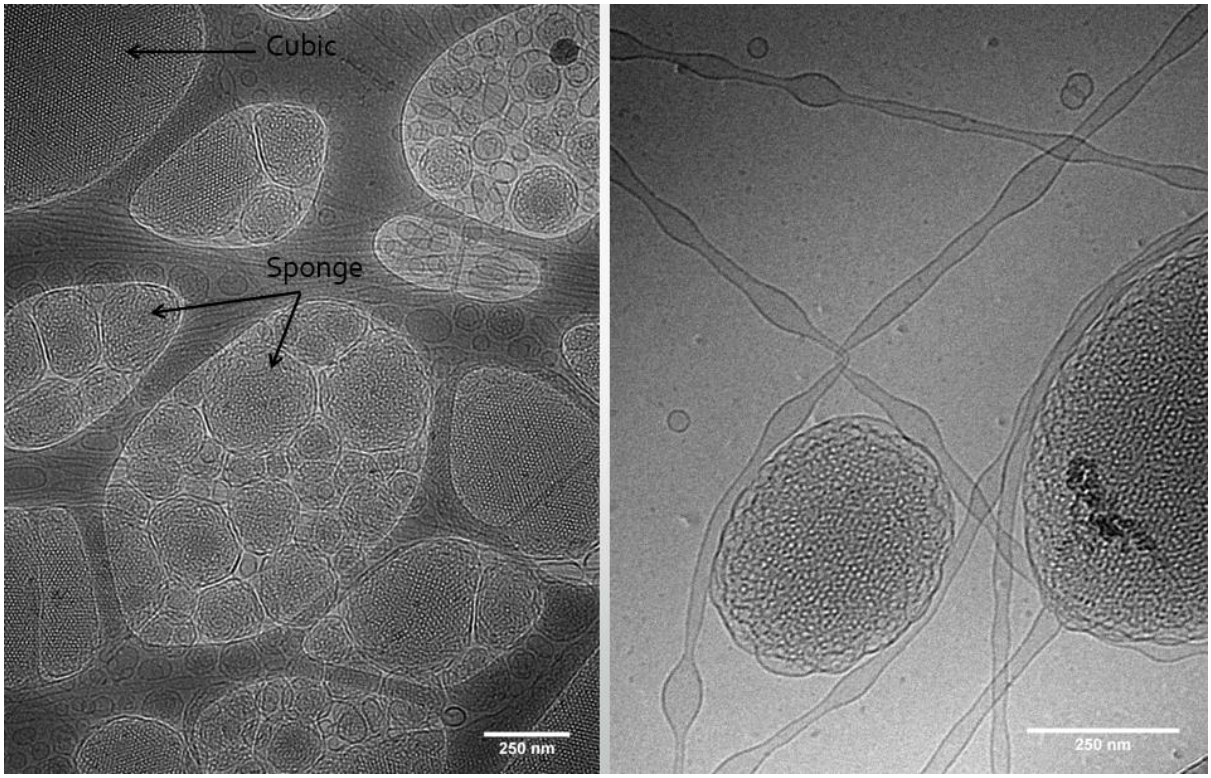

Figure 14. Tow images on the same sample but at different magnifications. The images show the sponge phase where the particle´s inside is in disordered for the sponge phase and ordered for the cubic phase. The elongated structures are caused by the sample plotting and have nothing to do with the LNPs.

However, the cryo-TEM images in Figure 15 are showing what the LNP with encapsulated protein looks like. The particles in images a) and b) have protein encapsulated and seem to not be in the sponge phase if it is compared with the sponge phase LNP in Figure 14. When the LNPs are encapsulated with the protein, the phase is different and not the sponge phase, see images 15a) and 15b). It is believed that the encapsulated LNPs have sponge phase structure, but the protein encapsulation drives the formulation of another phase elongated. Therefore, that protein attachment to the surface makes the SAXS measurement hard to be explained and it causes some extra X-ray scattering. On the other hand, image c) shows LNPs from the sample made in milli-Q water for the buffer effect tests. This image was taken a long time after the formulation which is why most of the LNPs were vesicles and had gone through a phase change. The image is showing that there are vesicles inside larger vesicles, that what is appears darker inside the LNPs. This phase is also confirmed by the SAXS measurements that had only one intensity peak which corresponds to the correlation thickness of the bilayer, see milli-Q water sample measurement in Figure 12.

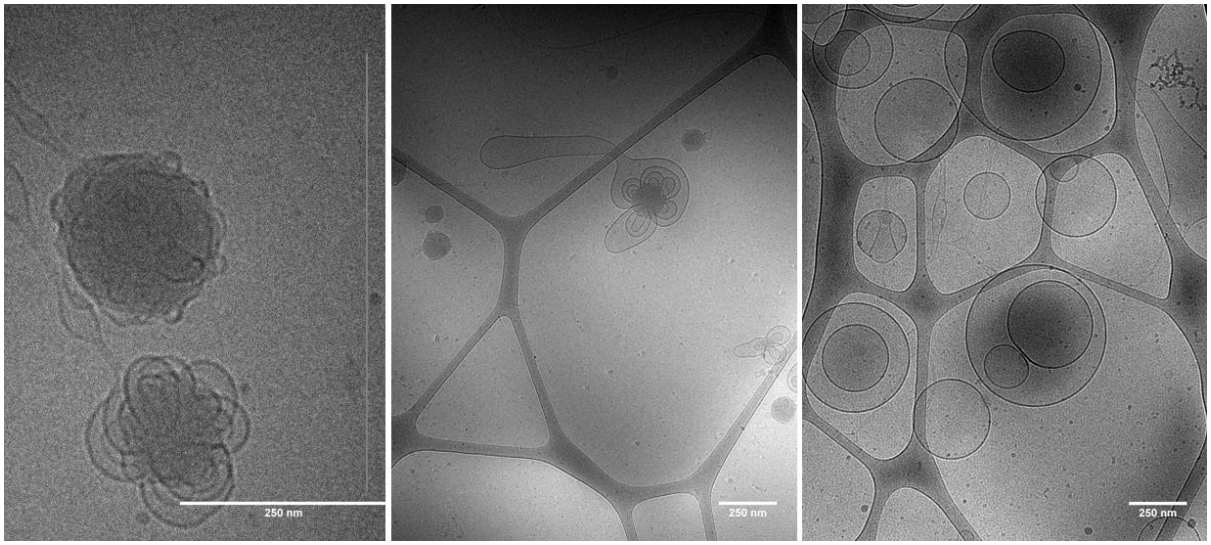

Figure 15. The cryo-TEM images. a) and b) are images of the protein encapsulated LNP with 1.6 mg protein/ml formulated at 300 µl/min. c) is an image on LNP formulated in milli-Q water from the buffer effect tests.

6. Conclusion

The microfluidics has been proven to be an effective method to formulate sponge phase lipid nanoparticles. The size of the LNP synthesised by microfluidics is influenced by the total flow rate, the flow ratio between the lipid and the buffer, and the amount of polysorbate-80 as a stabiliser. According to the fitting model, the flow rate decreases the size due to the short residence time that prevents the aggregation of lipids inside the channel. The higher flow ratio, which will result in low lipid concentration in the final product, leads to better mixing and therefore the lipids disperse into smaller LNP. Furthermore, and as other studies have shown, P80 helps forming stable sponge phase LNP and it drives the formulation of smaller particles. Compared to the standard dispersion made by sonication, microfluidics has a better performance to produce the sponge phase whereas the sonication damage the sponge phase LNP and drives the formation of vesicles instead. Moreover, the LNPs prepared by microfluidics were proven to have a sponge phase by the SAXS measurements.

In addition, the buffer and the pH have also an effect on the size and phase of the LNP. The results have shown that the pH=7 has a better sponge phase stability than higher pH-values. Thus, TRIS and PBS work better than milli-Q water when it comes to formulating smaller LNP. The sponge phase exists in all the buffers but must clearly in TRIS and PB at pH=7. When it comes to the stability of the size, LNPs in milli-Q water kept almost the same size after one month, which indicate high size stability, while in TRIS and PB the size has become larger.

However, microfluidics can also work for protein encapsulation of LNPs, but the amount of the encapsulated substance must not overcome the weight concentration of the lipid, because otherwise the LNP will not be able to be formulated in sponge phase. The absence of sponge phase has been proven by both SAXS and cryo-TEM.

References

1. Barriga H. M. G., Holme M. N., Stevens M. M.," Cubosomes; The Next Generation of Smart Lipid Nanoparticles", *Angew. Chem. Int. Ed.* **2019**, *58*, p. 2958-2978. DOI: https://doi.org/10.1002/anie.201804067
2. Nakama Y, "Chapter 15 – Surfactants", Editor(s): Robert Y. et al, *Cosmetic Science and Technology*, Elsevier, 2017, p. 231-244, ISBN 9780128020050, https://doi.org/10.1016/B978-0-12-802005-0.00015-X
8. Kulkarni C. V, et. al." Monoolein: a magic lipid?", *Physical Chemistry Chemical Physics* 2011, vol.13, no.8, pp 3004-3021. DOI: https://doi.org/10.1039/c0cp01539c
4. Rousseau D., et. Al. "Microemulsions as Nanoscale Delivery Systems", Editor(s): Murray Moo-Young, *Comprehensive Biotechnology*, Academic Press, 2011, p. 675-682, ISBN 9780080885049, https://doi.org/10.1016/B978-0-08-088504-9.00304-4
5. Spomenka M., Andreas Z., "*Glycerol monooleate liquid crystalline phases used in drug delivery systems*", International Journal of Pharmaceutics, vol. 478, 2015, p. 569-587. DOI: https://doi.org/10.1016/j.ijpharm.2014.11.072
6. Valldeperas M., et al. "*Sponge Phases and Nanoparticle Dispersions in Aqueous Mixtures of Mono- and Diglycerides*" Langmuir, 2016, vol. 32, p. 8650–8659. DOI: https://doi.org/10.1021/acs.langmuir.6b01356
7. Nasri N. A. M., et. Al, "*Effect of Concentration of Lipid with Surfactant and Ultra sonification Power on the Formation of Naringenin-Loaded Solid Lipid Nanoparticles*." Journal of Pharmaceutical Negative Results, v.13, p. 104–110. DOI: https://doi.org/10.47750/pnr.2022.13.S07.016
8. Kimura N., et. Al, "*Development of a Microfluidic-Based Post-Treatment Process for Size-Controlled Lipid Nanoparticles and Application to siRNA Delivery*", ACS Appl. Mater. Interfaces 2020, vol. 12, p. 34011–34020. DOI: https://doi.org/10.1021/acsami.0c05489
9. Schmitz K. S., "*CHAPTER 2 - Basic Concepts of Light Scattering*", Introduction to Dynamic Light Scattering by Macromolecules, 1990, p. 11-42, ISBN 9780126272604. DOI: https://doi.org/10.1016/B978-0-12-627260-4.50008-9
10. Bhattacharjee S., "*DLS and zeta potential – What they are and what they are not?*", Journal of Controlled Release, v. 235, 2016, p. 337-351, DOI: https://doi.org/10.1016/j.jconrel.2016.06.017 .
11. Krumrey, M., Small angle x-ray scattering (SAXS). *Characterization of Nanoparticles*, 2020, p. 173-183. DOI: https://doi.org/10.1016/B978-0-12-814182-3.00011-0
12. Angelov B., et. Al, "SAXS investigations of a cubic to a sponge L3 phase transition in self -assembled lipid nano carriers". Phys Chem Chem Phys, 2011; vol. 13 (8), p. 3073-81. DOI: 10.1039/c0cp01029d.
13. Honey G., et. Al," Chapter *3 - In vitro physicochemical characterization of nanocarriers: a road to optimization*", Editor(s): Prashant Kesharwani, Kamalinder K. Singh,

Nanoparticle Therapeutics, Academic Press, 2022, p. 133-179. DOI: https://doi.org/10.1016/B978-0-12-820757-4.00018-1 .

14. Ferriera C.J, "*Microfluidic methods for the controlled preparation of soft self-assembled nanocarriers for drug delivery*". Universidade do Minho. 2018. Online link: https://repositorium.sdum.uminho.pt/bitstream/1822/65059/1/10.%2BDissertacao%2B31343.pdf

Appendix A

ANOVA for Reduced Quadratic model.

Response 1: Particle size

Source	Sum of Squares	df	Mean Square	F-value	p-value	
Model	5549.47	7	792.78	17.27	0.0014	significant
A-Flowrate	351.13	1	351.13	7.65	0.0326	
B-[Lipids]	3444.01	1	3444.01	75.02	0.0001	
C-[Stabiliser]	60.17	1	60.17	1.31	0.2959	
AB	169.00	1	169.00	3.68	0.1035	
AC	756.25	1	756.25	16.47	0.0067	
BC	400.42	1	400.42	8.72	0.0255	
B^2	542.51	1	542.51	11.82	0.0138	
Residual	275.46	6	45.91			
Lack of Fit	102.79	4	25.70	0.2977	0.8607	not significant
Pure Error	172.67	2	86.33			
Cor Total	5824.93	13				

Factor coding is **Coded**.
Sum of squares is **Type III - Partial**

The **Model F-value** of 17.27 implies the model is significant. There is only a 0.14% chance that an F-value this large could occur due to noise.

P-values less than 0.0500 indicate model terms are significant. In this case A, B, AC, BC, B^2 are significant model terms. Values greater than 0.1000 indicate the model terms are not significant. If there are many insignificant model terms (not counting those required to support hierarchy), model reduction may improve your model.

The **Lack of Fit F-value** of 0.30 implies the Lack of Fit is not significant relative to the pure error. There is a 86.07% chance that a Lack of Fit F-value this large could occur due to noise. Non-significant lack of fit is good – the model is fitted.

Fit Statistics

Std. Dev.	6.78	**R^2**	0.9527
Mean	258.07	**Adjusted R^2**	0.8975
C.V. %	2.63	**Predicted R^2**	0.7460
		Adeq Precision	12.5197

The **Predicted R^2** of 0.7460 is in reasonable agreement with the **Adjusted R^2** of 0.8975; i.e. the difference is less than 0.2.

Adeq Precision measures the signal to noise ratio. A ratio greater than 4 is desirable. Your ratio of 12.520 indicates an adequate signal. This model can be used to navigate the design space.

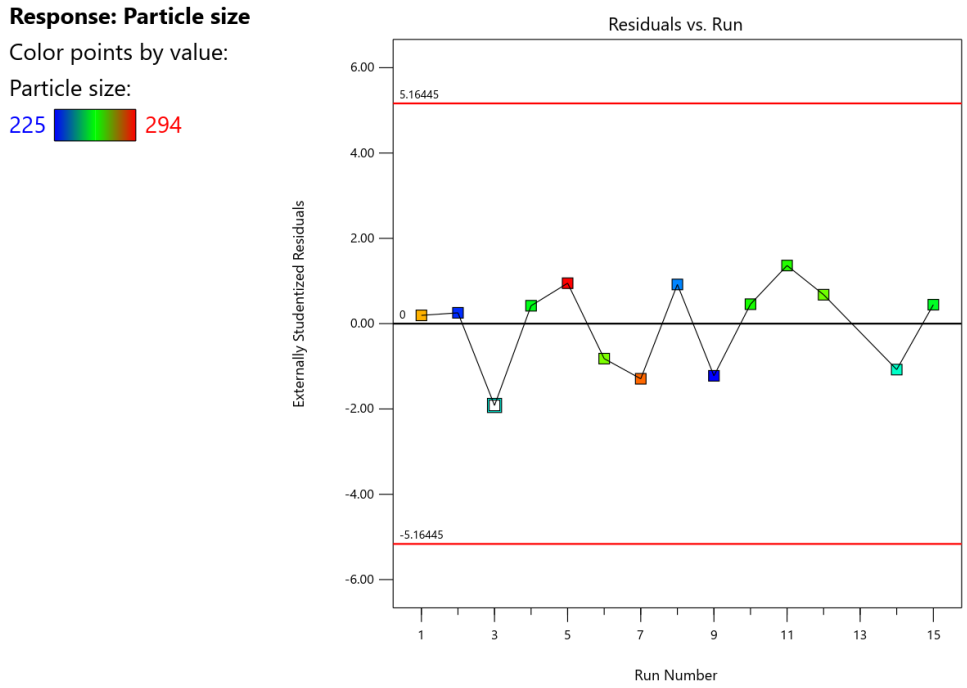

Figure 1A. The diversity of the measuring data against the residuals. It shows that all the measuring data lie within the range of the residuals.

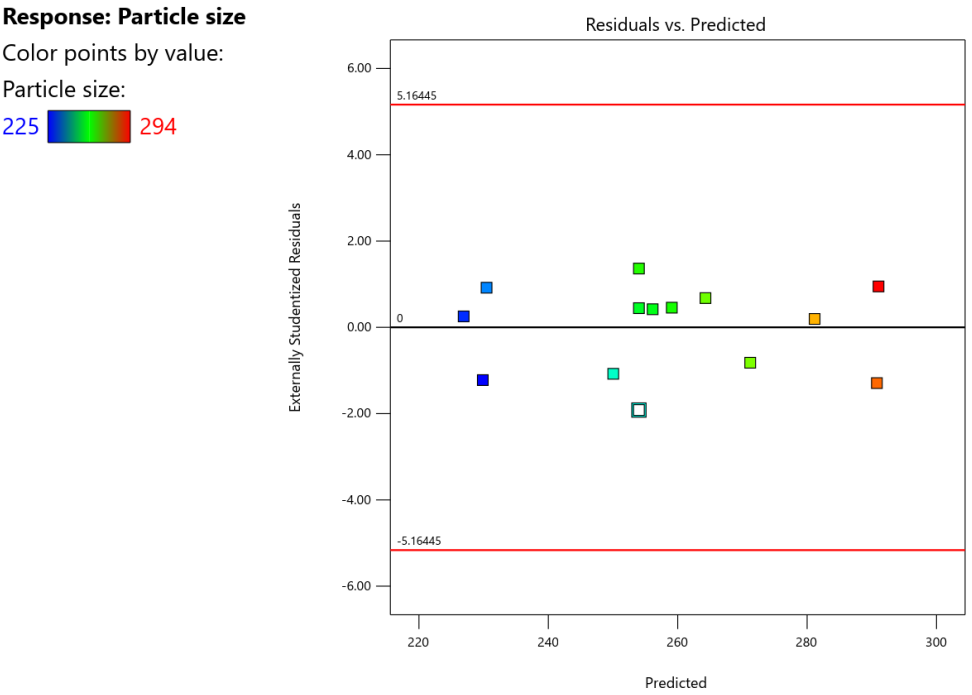

Figure 2A. The diversity of the predicted data by the model against the residuals. It shows that all the predicted data from the model lie within the range of the residuals.

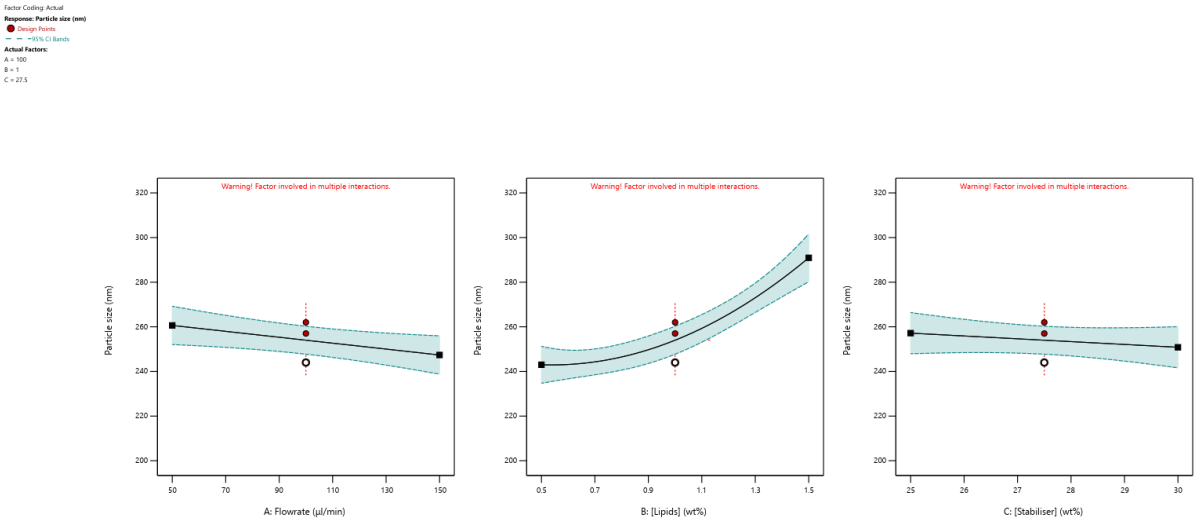

Figure 3A. The effect of each parameter if the other two are kept constant at F=100 µl/min, [L]= 1 wt% and [S]= 27.5 wt%.

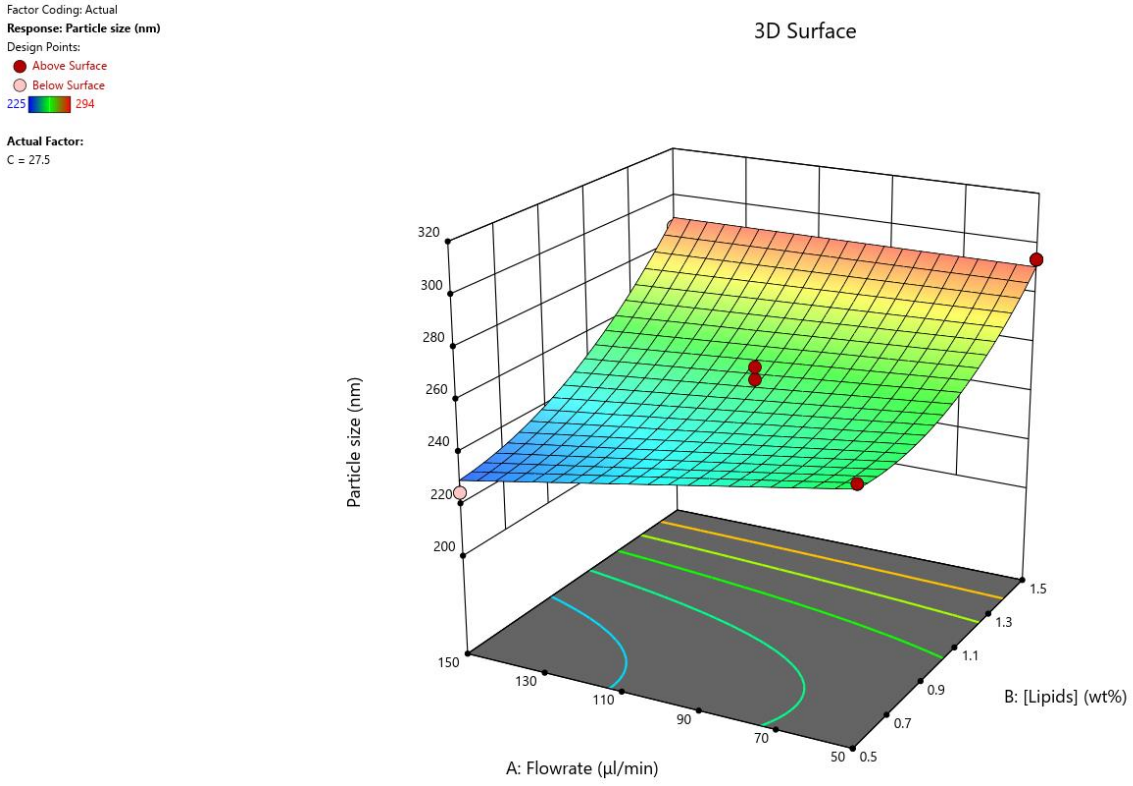

Figure 4A. The effect of the interaction between the total flow rate and the lipid concentration on the size of LNP if the [S]= 27.5 wt%.

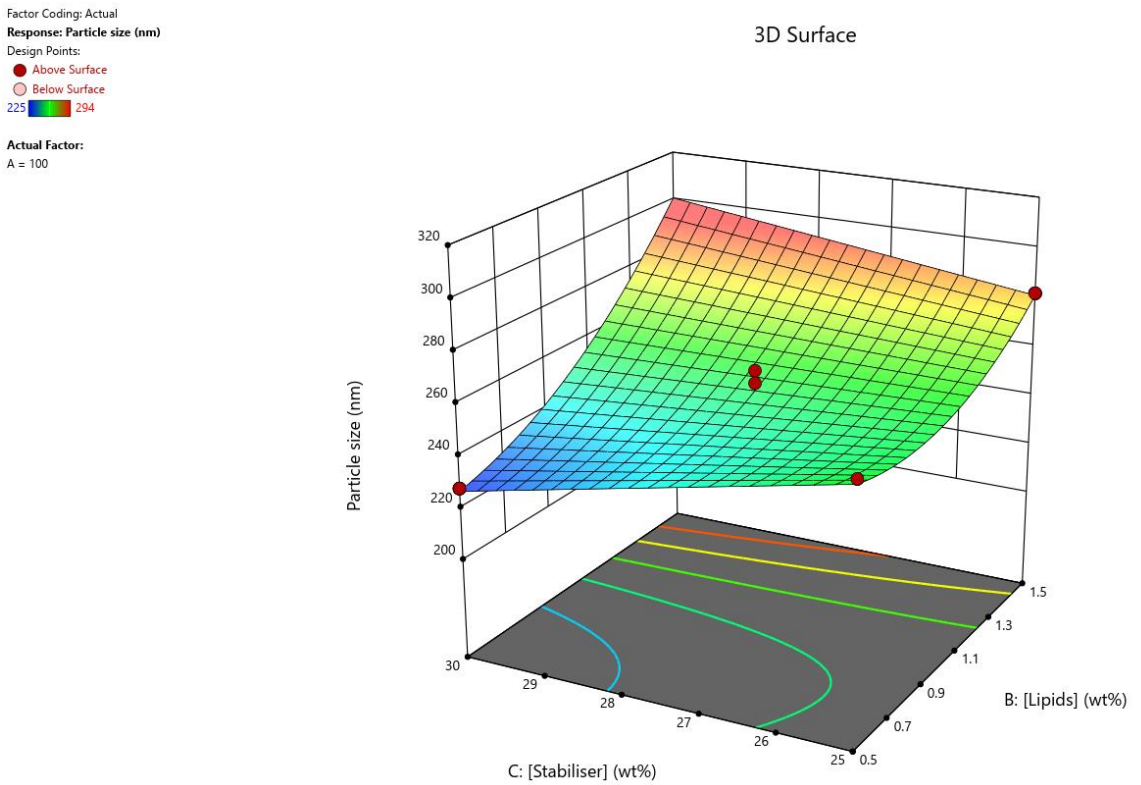

Figure 5A. The effect of the interaction between the stabiliser concentration and the lipid concentration on the size of LNP if the F= 100 µl/min.

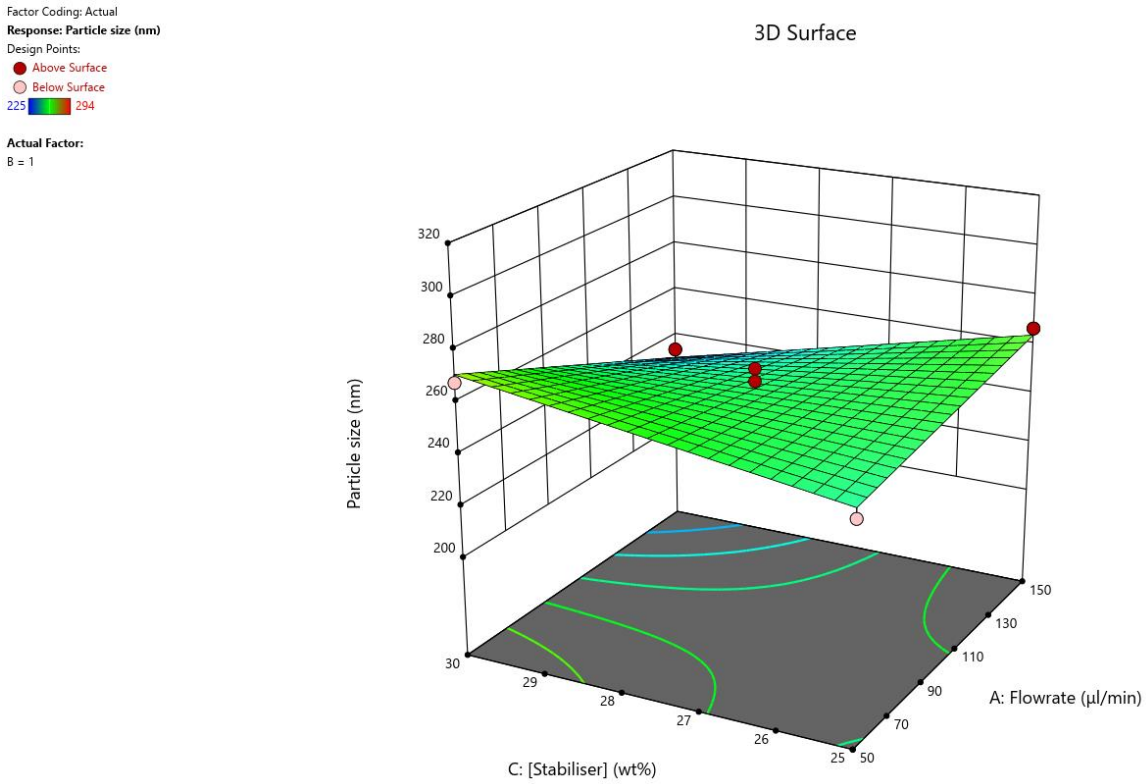

Figure 6A. The effect of the interaction between the stabiliser concentration and the lipid concentration on the size of LNP if the F= 100 µl/min.

Appendix B

Table 1B. The DLS measurements used to evaluate the ethanol removal method. The evaporation was based on which method provided a low PDI and stable size change. Both sample A and B was 40/60 wt% DGMO/GMO-50, sample A was with 25 wt% P80 and sample B was with 30 wt% P80. Both samples were made in microfluidics with the same condition, 200 µl/min and 1:9 flow ratio.

Sample	Z-avg	PDI
Sample A **Dialysis**	409.7±21	0,635±0.046
Sample B **Dialysis 5**	444.1±19.6	0.276±0.064
Sample A **Evaporation 8h**	256.8±2.01	0.32±0.067
Sample B **Evaporation 3h**	327.5±12.0	0.434±0.043

Table 2B. The measurements for the evaluation of the evaporation method and time needed for reaching a stable particle size. Sample A had 27.5 wt% P80 and was formulated at flow rate of 300 µl/min and flow ratio of 1:3. Sample B had 27.5 wt% P80 and was formulated at flow rate of 500 µl/min and flow ratio of 1:9. Both samples were diluted first by an adjusted factor to reach lipid concentration of 0.25 wt%. From the data, it can be seen that already after 2 hours, the LNPs size stops changing.

Sample	Z-avg	PDI
Sample A 1h evaporation	263±6.1	0.232±0.022
Sample A 2h evaporation	268.7±7.45	0.251±0.013
Sample A 3h evaporation	254.2±4.33	0.246±0.006
Sample A 4h evaporation	260.7±5.25	0.248±0.011
Sample B 1h evaporation	277.9±7.67	0.371±0.067
Sample B 2h evaporation	289.4±5.11	0.345±0.0669
Sample B 5h evaporation	280.5±2.6	0.311±0.008

Table 3B. The evaluation of the particle stability after the evaporation without dilution. Sample that has used in this test was formulated with total flow rate of 200 µl/min and with flow ratio of 1:9. The amount of P80 is 30 wt% of the lipids. The LNP are stable after 4 hours. That gave

us the conclusion that the evaporation with dilution before made the LNP stabler after shorter time.

Sample	Z-avg	PDI
1h	435.2±18.9	0.592±0.0478
2h	401.4±11.13	0.554±0.0820
3h	328.1±11.7	0.458±0.0238
4h	254.06±5.25	0.310±0.008
4.5h	246.2±3.83	0.299±0.016
5h	228.6±2.38	0.226±0.008